IEEE Access
Multidisciplinary ⋮ Rapid Review ⋮ Open Access Journal

Received January 18, 2021, accepted February 9, 2021, date of publication February 12, 2021, date of current version February 25, 2021.

Digital Object Identifier 10.1109/ACCESS.2021.3059418

Feasibility Study of Power Line Communications for Backhauling Outdoor Small Cells

JOSÉ ANTONIO CORTÉS[1], (Member, IEEE), FRANCISCO JAVIER CAÑETE[1], (Senior Member, IEEE), MATÍAS TORIL[1], EDUARDO MARTOS-NAYA[1], JAVIER PONCELA[1], LUIS DÍEZ[1], AND ALICIA GARCÍA[2]

[1]E.T.S.I. Telecomunicación, Departamento de Ingeniería de Comunicaciones, Universidad de Málaga, 29010 Málaga, Spain
[2]Vodafone Group Services Limited, Vodafone House, The Connection, Newbury, Berkshire RG14 2FN, U.K.

Corresponding author: José Antonio Cortés (jaca@ic.uma.es)

This work was supported in part by the Spanish Ministry of Ciencia e Innovación under Project PID2019-109842RB-I00.

ABSTRACT Small cells are low-power and low-range radio access nodes that can be used to increase network capacity in reduced areas with high traffic demand and to provide coverage to small isolated zones. As their number is expected to be very high, connecting them to the aggregation point in a cost-efficient manner is a key challenge, and there is consensus that none of the current technologies is valid for all scenarios. Since lamp-posts are one of the most convenient locations for outdoor small cells, this work analyzes the use of power line communications (PLC) over outdoor public lighting networks (OPLN) as a backhaul technology for outdoor small cell deployments. To this end, the characteristics of the PLC channels established in OPLN are firstly assessed. The analysis combines noise measurements performed in existing OPLN and channel responses obtained from a multiconductor transmission line (MTL) model. The attenuation, delay spread and spatial correlation of the multiple-input multiple-output (MIMO) channels are investigated and their influence in the physical layer parameters of PLC systems is discussed. Afterward, the performance achieved by state-of-the-art PLC systems is assessed. To this end, estimations obtained by means of simulations and measurements taken in actual networks are included. Data throughput achieved by PLC systems based on the ITU-T G.hn standard, as well as the expected improvements obtained by 3×3 MIMO systems, are given. Results indicate that PLC can be an interesting technology for coverage-driven small cell deployments with backhaul length shorter than 150 m, offering throughput values similar to existing Sub-6 GHz wireless solutions in non-line-of-sight (NLOS) conditions and wired ones like G.fast.

INDEX TERMS Power line communications, backhaul, small cells, outdoor public lighting networks.

I. INTRODUCTION

Mobile data traffic has been annually increasing by approximately 30% in the last six years. This trend is expected to continue in the near future, with an expected growth factor close to 5 in the term 2019-2025 [1]. Most of this traffic will be due to fourth generation (4G) system connections, which in 2019 exceeded the aggregated value of the remaining generations, and that by 2023 are expected to represent about 46% of the total mobile connections, while fifth generation (5G) ones will be about 10.6% [2].

Three main strategies are used to accommodate this enormous demand. A first one improves physical layer (PHY) procedures by introducing denser constellations and full dimension multiple-input multiple-output (MIMO) techniques at the base station (BS), just to name a couple of examples.

Another strategy is to extend the employed bandwidth. To this end, millimeter wave (mmWave) bands above 24 GHz have been allocated to 5G and the unlicensed spectrum at 5 GHz is being used in Long Term Evolution (LTE) [3]. Two different approaches can be employed for the latter: to use Wi-Fi as radio technology in the unlicensed band and aggregate it with the LTE flow used in a licensed one, as in LTE-WLAN Aggregation (LWA), and to use LTE Radio

The associate editor coordinating the review of this manuscript and approving it for publication was Jiafeng Xie.

Access Network (RAN) also in the unlicensed band, as in Licensed Assisted Access (LAA) [4]. Interestingly, the use of both mmWave and 5-GHz bands require small cell sizes because of the higher propagation loss.

The third strategy is to increase the density of BS, which is usually referred to as network densification [5]. However, the deployment of macro cells is expensive. In addition, the density of macro cells per km^2 in some urban areas is causing a serious shortage of available sites. Moreover, the concern about macrocellular BS radiation is leading municipalities to restrict the installation of new towers. Hence, small cells with low-cost and low-power BS, with coverage range from tenths to several hundred meters, offer a simpler cost-effective alternative to this end. Small cells can be used both to increase network capacity in congested hotspots and to provide coverage to rural isolated localities with no macrocell coverage [6].

Note that two out of the three above strategies rely on the deployment of small cells. In fact, these are considered a key enabling technology for 5G networks and its number is forecasted to become an order of magnitude larger than the current number of macrocells [6]–[8]. In the case of outdoor small cells, the availability of a cost-efficient connection to the first point of aggregation, usually referred to as (last mile) backhaul, is of paramount importance. Since the backhauling system may represent about 50% of the total cost of ownership (TCO) of small cell deployments [9], mobile network operators (MNO) consider sites and backhaul costs as the main barriers for network densification [10].

Many wireless and wired alternatives have been considered for the backhaul. The former encompasses microwave, mmWave and even free-space optical (FSO) for line-of-sight (LOS) links and sub-6 GHz solutions for non-line-of-sight (NLOS) ones. Satellite and television white space (TVWS) are also being considered. Alternatively, wired technologies include fiber optic-based solutions, digital subscriber line (DSL) and hybrid fiber-coax technologies such as data over cable service interface specification (DOCSIS). However, it is well accepted that no solution is valid for all scenarios. The reader is referred to [6], [11] and references therein for detailed analyses of the referred backhaul technologies.

Lamp-posts are one of the most convenient location for outdoor small cell BS [6], [12]. They are widely spread in public spaces and connected to the mains electricity (generally by means of underground conduits). In this context, the use of power line communications (PLC) over outdoor public lighting networks (OPLN) as backhauling technology may be a cost-effective solution, since the equipment, infrastructure and leasing costs are very small [13]. Indeed, it is currently being used as a backbone for video surveillance cameras and Wi-Fi hot spots [14].

The term PLC denotes a set of technologies in which information is conveyed through the electrical wires. PLC systems are commonly classified according to the employed bandwidth into narrowband (NB), using frequencies up to 500 kHz, medium band (MB), transmitting in the band up to 12 MHz, and broadband (BB), using frequencies up to 100 MHz. NB and MB are mainly used in industrial and Smart Grid applications [15], [16]. BB PLC systems have been mainly used for in-home multimedia services, although they are also used in Smart Grid. By employing multicarrier modulations, adaptive bit-loading, MIMO techniques and strong coding schemes, state-of-the-art BB PLC achieve PHY throughput values around 1.5 Gbit/s [17]. Further performance gains can be achieved, for instance, by exploiting the non-Gaussian nature of the noise [18] and its correlation in certain frequency bands [19], by using in-band full duplex (IBFD) techniques [20] and other medium access control (MAC) improvements [21]. This article focuses on BB PLC systems for outdoor small cells, hereafter referred simply to as PLC and small cells, respectively.

In this context, the use of PLC over the medium-to-low voltage (MV/LV) network and the modeling of the traffic to be backhauled has already been explored in [22]. This work focuses on assessing the characteristics of PLC channels established in OPLN and evaluating the capability of PLC systems to fulfill the requisites of the backhaul for different small cell uses cases. It makes two main contributions:

- The characteristics of PLC channels in OPLN are qualitatively and quantitatively described. The study combines noise measurements accomplished in actual networks with a multiconductor transmission line (MTL) modeling of the channel response.
- Performance values achieved by state-of-the-art PLC systems are given. The study includes both simulated and measured results. Moreover, expected values obtained by using 3×3 MIMO systems are also provided.

Presented results can be of interest for MNO and PLC system manufacturers and researchers. The former can benefit from the detailed analysis of the actual performance (and expected improvements) of PLC when used for outdoor small cell backhauling. They can also use the methodology employed in this work as part of their backhaul planning toolkit to assess the feasibility of PLC in a given scenario. For the PLC community, an interesting scenario with an enormous potential growth is presented, which poses rather different challenges to the conventional indoor scenario.

Preliminary results of this work were presented in [23]. This article extends the referred conference paper by adding the following elements: 1) an improved contextualization of the problem which details the requisites the backhaul has to fulfill in the different small cell use cases; 2) both the analysis of OPLN PLC channels and the throughput assessment are extended to include MIMO systems; 3) measured throughput, delay and jitter values obtained in actual networks are given; 4) a review of techniques that are currently being investigated and might enhance the performance of PLC systems for the considered application is made and their potential improvement is discussed.

The rest of this article is organized as follows. The requisites of the backhaul for the different small cell uses cases are

reviewed in Section II. A review of the state of the art in PLC is given in Section III. Then, the elements and structure of OPLN and the channel model proposed to estimate the performance by means of simulations are presented in Section IV and Section V, respectively. Estimated and measured performance values are given in Section VI. It also discusses expected performance improvements that can be obtained by incorporating some innovative techniques recently proposed in the literature. Finally, Section VII recapitulates the main aspects of the work.

II. OUTDOOR SMALL CELL BACKHAUL REQUIREMENTS

The throughput required for the backhaul depends on a large number of parameters given by the service offered by the small cell, e.g., channel bandwidth, densest constellation, MIMO order, use (or not) of carrier aggregation, cell load and RAN architecture, among others. Two types of RAN schemes can be considered: a centralized one, in which multiple radio units are connected to a central node, where baseband processing is performed; or a distributed RAN architecture. Although the centralized scheme allows an improved interference management, the required throughput is disproportionately high for most existing backhaul technologies and a distributed RAN architecture is commonly deployed [24], [25]. From now on, this is the assumed scheme.

A. THROUGHPUT AND DELAY

Small cells support both the S1 interface, which enables communication with the packet core, and the X2 interface, which allows direct connection with other small or macro cells [26]. Hence, the backhaul traffic of an LTE small cell consists of both the S1 and X2 user and control plane information, the transport protocol overhead, the IPsec overhead and other minor components employed for operation and maintenance (O&M) and synchronization [27]. The largest component of the backhaul traffic corresponds to the user plane (the control plane traffic may only reach about 25% of the former), which is conveyed to the serving gateway (S-GW) using a protocol stack with user datagram protocol (UDP) as transport protocol [28].

Two cell loads conditions are considered in order to estimate the bit-rate that has to be backhauled: busy times and quiet times. During the former, many users are distributed across the cells, experiencing significantly different signal quality. During quiet times, only one user with good link quality is assumed to be accessing each cell. Since all cell resources are allocated to a user with high signal to noise ratio (SNR) and there is low interference from other cells, the cell spectral efficiency and throughput are larger than when resources are shared among users with diverse signal quality [27]. Hence, the quite time load condition represents the most demanding scenario for the backhaul.

The report in [27] estimated quite period bit-rates of 188 Mbit/s and 63 Mbit/s in the downlink (DL) and uplink (UL), respectively. The corresponding values for the busy times are 34 Mbit/s and 24 Mbit/s, respectively.

TABLE 1. Categorization of Backhaul Technologies in 3GPP TR 36.932 [31].

Backhaul technology	Latency (ms) one way	Throughput	Priority [a]
Fiber 1	10–30	10 Mbit/s–10 Gbit/s	1
Fiber 2	5–10	100 Mbit/s–1 Gbit/s	2
Fiber 3	2–5	50 Mbit/s–10 Gbit/s	1
DSL	15–60	10 Mbit/s–100 Mbit/s	1
Cable	25–35	10 Mbit/s–100 Mbit/s	2
Wireless	5–35	10 Mbit/s–100 Mbit/s[b]	1

[a] 1 is the highest

[b] Typical values, but may be up to the Gbit/s range

However, it assumed an LTE Release 8 small cell using a 20-MHz bandwidth with 2 × 2 MIMO and category 4 user equipments (UE) with maximum DL and UL bit-rates of 150 Mbit/s and 50 Mbit/s, respectively. These values are doubled for newer category 7 UE introduced in Release 10. Hence, the resulting DL and UL bit-rates would be 375 Mbit/s and 126 Mbit/s, respectively, for the quite times and 68 Mbit/s and 48 Mbit/s for the busy times (assuming the same overhead as in Release 8).

Release 10 and subsequent ones include additional features to increase the bit-rate, like carrier aggregation and higher order MIMO [3], [29]. However, the power and form factor constraint of small cell BS will likely preclude the use of very high capacity configurations in small cells. In fact, other works assume lower bit-rates than the ones indicated above for small cell backhauling analysis [25]. Moreover, it has been shown that under provisioning the backhaul capacity, within certain range, yields a negligible impact on the user quality of experience (QoE) [6].

Regarding delay requirements, the 3rd Generation Partnership Project (3GPP) defines end-to-end packet delay budgets for different service types of the user plane [30]: 50 ms for gaming, 100 ms for voice, 150 ms for live streaming video and up to 300 ms for buffered streaming video. These values must be doubled when translated to round trip delays and encompass the processing and transmission delays of all the network elements (UE, BS, packet core processing delay, etc.), which according to the estimation in [6] may be up to 40 ms (round trip). Hence, the maximum round trip delay for the small cell backhaul is 60 ms for gaming services, 160 ms for voice and may exceed this value for other services.

The aforementioned throughput and delay requisites may not be achieved in certain scenarios. In fact, the 3GPP has categorized backhaul solutions, based on MNO input, as shown in Table 1 [31].

B. SMALL CELL USE CASES

The requisites of the backhaul depend on the aim of the small cell deployment, which can be roughly classified into capacity and coverage driven scenarios. The former is typically aimed at increasing capacity in dense urban congested spots and enhancing the QoE by improving the data rate in high traffic demand areas. Hence, the peak bit-rate of

TABLE 2. Small Cell Backhaul Requisites for the Capacity and Coverage Use Cases for Release 8-Category 4 and Release 10-Category 7 UEs.

Use case	Minimum UL+DL Throughput (Mbit/s) Rel.8-Cat.4 | Rel.10-Cat.7	Maximum round trip delay (ms)
Capacity	251 | 501	60 –160
Coverage	58 | 106	

the small cell should not be limited by the backhaul capacity [27]. The latter use case is targeted at providing network coverage to isolated towns and villages with no macrocell coverage, but also for enhancing urban spots coverage of MNOs with no allocated spectrum below 1 GHz [6], [32]. It also includes situations where mobile services have to be rapidly deployed in a given spot. In this use case, the backhaul capacity can be relaxed and provisioning for the busy time is acceptable [27], [33].

Table 2 summarizes the throughput and delay requirements set as reference in this work for each use case. These values correspond to an individual cell but, interestingly, when a set of C cells are connected to the same backhaul, the required capacity can be estimated as max (quite time bit-rate, $C \times$ busy time bit-rate), since busy times tend to occur simultaneously, but it is unlikely that peak bit-rates are demanded at the same time in all cells [6].

There is agreement that none of the existing backhaul technologies is valid for all scenarios. Moreover, the study in [32] concludes that, from a business perspective, the optimum solution is to change the mix of backhaul technologies used throughout the lifecycle of the deployment, trending to more expensive installations as the network matures and higher capacity is demanded.

III. REVIEW OF PLC TECHNOLOGY

This section summarizes the main characteristics of state-of-the-art PLC systems, describing their upper performance bound and their most relevant parameters, which will be used in Section VI to estimate the achievable throughput in OPLN. The reader is referred to [34]–[36] for more detailed reviews.

Initial PLC systems, based on industry alliances specifications, used the frequency band up to 37.5 MHz and achieved PHY bit-rates around 200 Mbit/s [37]. They were mainly designed for in-home applications, although they are also used in outdoor Smart Grid applications [36, Ch. 9].

The three state-of-the-art PLC systems currently found in the market are designed according to the HomePlug AV2 industry specification [38], the IEEE P1901 standard [39] and the ITU-T G.hn standard [40]–[43]. They are non-interoperable but implement the inter-system protocol (ISP) for coexistence [44]. While HomePlug AV2 and ITU-T G.hn are oriented to in-home applications ('hn' actually stands for home networking), IEEE P1901 also includes features for access applications, being currently used in Smart Grid [45].

HomePlug AV2 and ITU-T G.hn define windowed orthogonal frequency division multiplexing (OFDM)-based systems, while IEEE P1901 defines two non-interoperable PHY, one based on windowed OFDM and another on wavelet OFDM. Table 3 summarizes their main PHY parameters.

TABLE 3. Main PHY Features of State-of-the-Art PLC Systems.

Parameter	HomePlug AV2	ITU-T G.hn	IEEE P1901 OFDM | wavelet
Frequency band (MHz)	100	100	50
Number of carriers[(a)]	4096	4096	2048 | 1024
Intercarrier spacing (kHz)	24.414	24.414	24.414 | 47.07
Min–max guard interval (μs)	0–47.12	1.28–10.24	1.6–47.12 | -
Rolloff interval (μs)	4.96	5.12	4.96 | -
Min–max number bits per symbol	1–12	1–12	1–12 | 1–5
Coding rates	1/2, 16/21, 16/18	1/2, 2/3, 5/6, 16/18, 20/21	1/2, 16/21, 16/18 | $[\frac{40}{56}, \frac{239}{255}] \times \frac{k}{k+1}$ [(b)]
MIMO[(c)]	2×3	2×3	-

[(a)] The number of active carriers is actually lower and determined by the electromagnetic compatibility regulations indicated below.

[(b)] Two possible Reed-Solomon rates and convolutional code with $k = 1, \ldots, 7$.

[(c)] Typical values, but up to 2×4 could be employed.

As seen, the three windowed OFDM-based systems use the same intercarrier spacing, 24.414 kHz and bit-loading with up to 4096-quadrature amplitude modulation (QAM). However, IEEE P1901 operates below 50 MHz, whereas HomePlug AV2 and ITU-T G.hn can employ the frequency band up to 100 MHz, although, in practice, only frequencies below 86 MHz are used in most countries to avoid interfering with the frequency modulation (FM) broadcasting. Furthermore, the former does not have MIMO capabilities, while the HomePlug AV2 and ITU-T G.hn do.

All these systems define a time division multiple access (TDMA)-based MAC which can use both a connection oriented, contention-free service, and a connectionless service based on carrier sense multiple access/collision avoidance (CSMA/CA).

The bit-rate achieved by PLC systems in actual channels is strongly dependent on the power spectral density (PSD) and the frequency band of the transmitted signal. These are limited by electromagnetic compatibility (EMC) regulations, which vary among regions[1] [46]. In the United States (US), PLC transmissions are regulated by the Federal Communications Commission (FCC) under the Electronic Code of Federal Regulations, Title 47, Part 15. It specifies limits for

[1]For instance, Japan is one of the most restrictive countries, with PLC transmissions allowed only in the frequency band below 30 MHz and for in-home scenarios. Hence, results provided in this work are not currently applicable to this country.

radiated emissions [47], which are commonly interpreted to allow transmissions in the 1.8–30 MHz range with a PSD of −50 dBm/Hz and in the 30–86 MHz band with a PSD of −80 dBm/Hz [34], although slightly more stringent limits are interpreted in [48].

In the European Union (EU), in-home single-input PLC transmissions are regulated by the EN50561-1 in the 1.6–30 MHz range and by the EN50561-3 in the 30–80 MHz band [49], [50]. Accordingly, the PSD employed by ITU-T G.hn systems is defined in the ITU-T Rec. G.9964 [43] and allows injecting −55 dBm/Hz in the range 2–30 MHz and −85 dBm/Hz in the range 30–80 MHz, with gaps to avoid interference to existing services, e.g., aeronautical, radio amateurs, radio astronomy. While there is no specific regulation for access applications, PLC systems are employed in outdoor applications relying on EU Directive 2014/30/EU [45], [51], [52].

As a result, current ITU-T G.hn and HomePlug AV2 chipsets achieve maximum PHY bit-rates around 1.5 Gbit/s [38, pp. 61] [17] and UDP ones around 1 Git/s [53], while IEEE P1901 achieve maximum PHY bit-rates around 500 Mbit/s. Despite these rates are computed in an ideal scenario, the comparison with the throughput requirements given in Table 2 suggests the interest in assessing PLC as a backhaul technology, at least for certain small cell scenarios.

IV. OUTDOOR PUBLIC LIGHTING NETWORKS (OPLN)

This section firstly describes the elements and structure of OPLN and then presents the particular networks used in this work to assess the performance of PLC systems.

A. NETWORK STRUCTURE

OPLN consist of a control panel from which a series of circuits are deployed. The input to the control panel are the power lines coming from the MV/LV transformer. Three-phase circuits consisting of three conductors, one for each phase, and an additional one for the common neutral are generally used. Phases are generally named L1, L2 and L3, although R, S, and T are still used in many European countries. Lamps are alternatively connected between phases L1, L2, L3 and the neutral, in order to get a balanced network. Monopolar and 4-pole cables, deployed inside a common conduit, are employed. Fig. 1 depicts an example network. While the same type of cabling is usually employed in all the circuits of an OPLN, a different one is assumed in Fig. 1 for generality.

The last two lamps of each circuit generally have a lower number of conductors when monopolar cables are used. As shown in circuit 1 in Fig. 1, typically only one phase reaches the last lamp of the circuit and two phases the penultimate one. When 4-pole cables are used, the three phases reach all lamps. However, only one is generally active (i.e., connected to the mains) at the last lamp and two at the penultimate, as in circuit 2 in Fig. 1. This avoids having the mains in conductors sections that do not use it.

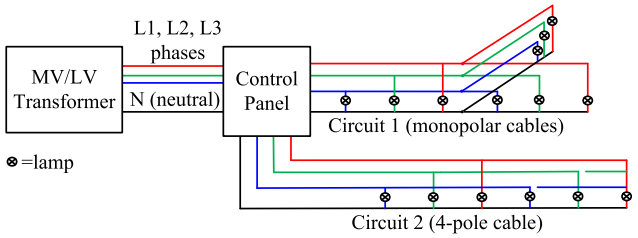

FIGURE 1. Structure of an example OPLN with two circuits.

In a small cell deployment, the aforementioned situation has to be taken into account if the BS is placed in the last or penultimate lamp-post of a circuit, since the MIMO capability of the PLC system is compromised. Nevertheless, the problem can be solved straightforwardly if 4-pole cables are used, just by joining the existing conductors. Additional cables have to be deployed if monopolar cabling has been employed. However, the cost of the latter is small because conduits are already deployed.

Control panels are usually located in the sidewalk and contain metering, control and protection devices. Activation of lighting is done by either a central controller or an astronomical clock that computes sunrise/sunset times on a daily basis. Protection devices usually consists of a general power control switch, magneto-thermal protection cutout and differential circuit breaker. These same devices are also installed in each circuit. The high number of protection devices will increase the attenuation of PLC signals between circuits. According to [54], attenuation values well in excess of 40 dB can be expected. This has two opposing effects: it reduces the interference between PLC devices connected in different circuits but makes almost unfeasible to communicate PLC devices connected to different circuits.

In many countries, OPLN must reduce their luminous intensity in the small hours of the night. This is done either on a lamp by lamp basis, using remotely controlled electronic ballasts, or in a centralized manner using a flux reducer stabilizer (FRS). The latter reduces the luminous intensity by lowering the mains voltage in the circuits, usually by about 20%. Hence, it must be ensured that both the small cell BS and the PLC devices are able to operate at this reduced voltage. Moreover, measurements performed in this work show that the FRS has a very low impedance: below 20 Ω in almost all the frequency band. Since this impedance will be in parallel with the communication device, it will absorb much of the communication signal power. Therefore, when an FRS is used, the control panel should be avoided as one of the communication end points.

B. NETWORK TOPOLOGIES

OPLN are designed taking into account both luminous and electrical criteria. The former depend on street width and determine the deployment structure (one-sided, two-sided in staggered rows or two-sided in facing rows/central deployment), the lamp separation, lamp power and lamp-posts height. The electrical criteria determine the cable section,

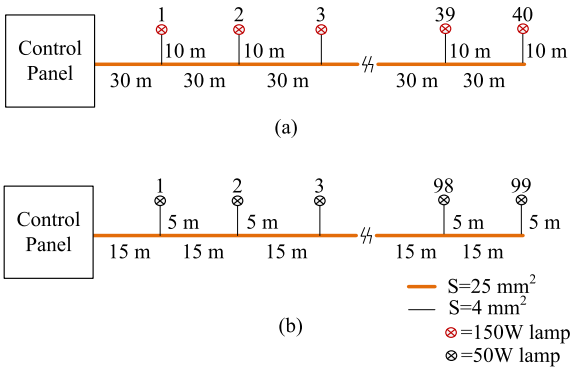

FIGURE 2. (a) Linear topology 1, consisting of 40 lamps spaced 30 m (b) Linear topology 2, consisting of 99 lamps spaced 15 m.

the maximum number of lamps per circuit and the maximum cable length. The latter is imposed to guarantee that the voltage drop at the circuit end due to the resistive loss of the conductor is kept below a certain range (typically 3%).

Circuits usually have a tree-like topology, with a more linear or branched shape depending on street characteristics. For the purpose of this work, the following three types of network topologies are considered. They have been designed according to the Spanish specifications [55]–[57].

1) EXTREME CASE TOPOLOGIES

Communication system performance decreases as the channel attenuation increases. In PLC channels, attenuation augments with:

- Link length, due to the skin effect of the conductors and to the losses in the cable dielectric. Since both effects increase with frequency, they cause the frequency response to have a low-pass profile.
- Number of derivations (to lamps or to branches of the circuit) from the main path from transmitter to receiver, which cause multipath propagation because of the impedance mismatch. As a result, the channel frequency response exhibits notches.

Two extreme cases of network topologies have been defined by analyzing common rules in the design of OPLN: 1) linear topologies consisting of very long circuits without branches, which model large avenues, seafronts, etc. and 2) highly branched topology corresponding to a Manhattan-like grid, which models a two-dimensional urban scenario. Based on this observation, the following two sets of topology instances have been defined:

1) Linear topologies. This set comprises two topologies that model a 2-lane street, one with 40 lamps (150 W) and lamp-posts 10 m high, and another with 99 lamps (50 W) and lamp-posts 5 m high. Fig. 2 depicts their layout, where S denotes cable section.
2) Manhattan-like topology. Fig. 3 shows its structure, whose dimensions have been taken from the Ensanche district in Barcelona (Spain).[2] This network is unrealistically large because of its sensitivity to faults in the main cable or the control panel. However, it can be useful for assessing the performance of PLC system.

[2]See corresponding map at https://cutt.ly/ogEZpcF

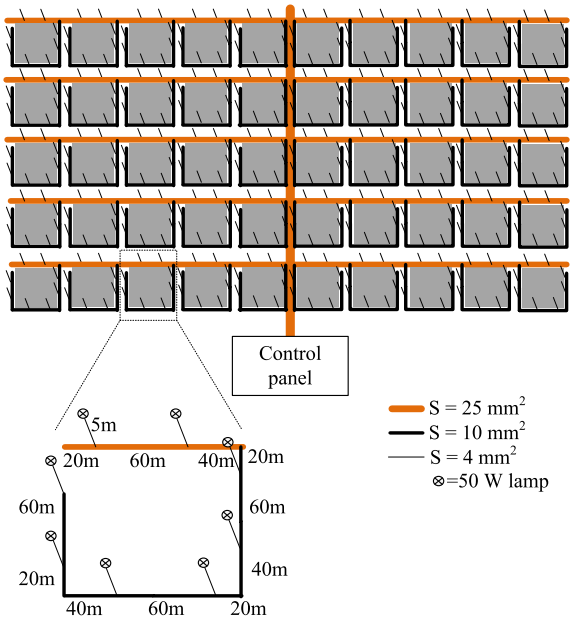

FIGURE 3. Branched network with a Manhattan-like topology.

2) RANDOM TOPOLOGIES

To obtain a larger number of realistic irregular topologies with a wide range of characteristics, a random topology generator has been developed. It takes into account both physical and electrical parameters (street width, cable section) and the design rules used in common practice (deployment structure, lamp-post distance and lamps power).

As mentioned, OPLN have a tree-like structure with a number of hierarchical layers. The tree is generated from the root (control panel) to the leaf nodes (lamps). At each node, a number of branches $(0, 1, 2, \ldots, N_{\text{bmax}})$ are generated with probability given by a Galton-Watson process [58]. Once the tree network structure is built, a random distance is assigned to each branch. Distances range from 0 to the maximum distance of a straight segment (i.e., without branches) still satisfying the voltage drop constraint. However, even if all branches satisfy the voltage drop constraint individually, it might happen that, due to the voltage drop in parent segments, the overall voltage drop constraint from the control panel is not met. Thus, the algorithm computes the accumulated voltage drop from root to children and then eliminates segments that do not satisfy the constraint. Fig. 4 shows an example topology generated according to this procedure.

Six random topologies have been taken from a large set of generated networks by manually selecting those with rather different topologies. Hereafter they will be referred to as *Random 1*, *Random 2*, …, *Random 6*. The corresponding number of lamps of each topology is 15, 19, 21, 22, 26 and 27.

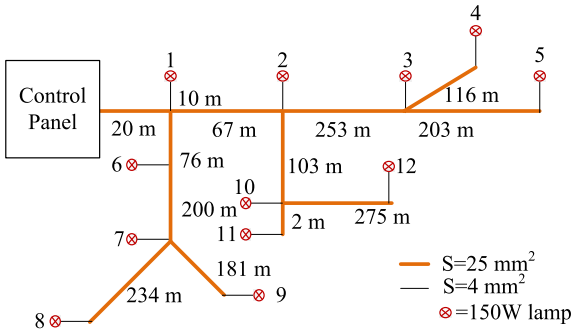

FIGURE 4. Layout of a random topology obtained with the developed generator. All lamp-posts are 10 m high.

3) REAL TOPOLOGIES

Finally, two actual networks layouts provided by the City Council of Málaga (Spain) have been employed. One corresponds to the Aurora avenue (with a more linear structure) and other to the SOHO district (with a more branched structure).[3]

V. CHANNEL CHARACTERIZATION

To assess the performance of PLC systems over OPLN channels, both the channel response and the noise have to be characterized. The former has been estimated by using a bottom-up modeling strategy based on MTL [59], as traditionally done in indoor PLC scenarios [60], [61]. A large set of statistically representative channels has been obtained by applying this technique to the selected topologies employing typical cable parameters.

Noise has been characterized by performing measurements in actual OPLN, since, to the best authors' knowledge, neither published models nor empirical results are available in the literature for this scenario.

A. CHANNEL RESPONSE

The response of the channels in the network topologies described in Section IV-B has been obtained by applying the MTL modeling approach detailed in [61]. The transmitter and receiver are located at street light positions and the control panel is never employed to this end because of the low impedance of the FRS mentioned in Section IV-A. Three type of channels have been obtained at each transmitter-receiver location: a single-input single-output (SISO), a 2×2 MIMO and a 3×3 MIMO channel. While PLC systems defined in ITU-T G.hn do only consider two transmitting ports, the number of conductors used in OPLN allows using one additional transmitting port, which will likely improve the performance. In the MIMO case, the transmitter and receiver circuits are modeled as in [61]. The resulting number of useful channels (of each type) is shown in Table 4.

Fig. 5 depicts some representative SISO channels from the Linear 1, SOHO and Manhattan-like topologies with different link lengths, ℓ, in meters. As seen, all channels have a remarkable low-pass behavior due to the high frequency loss caused by the skin effect and the dielectric losses. Notches due to the multipath effect are observable only in the low frequency range (below 20 MHz), where the attenuation due to the skin effect and the dielectric is not so important. This contrasts to indoor PLC channels, where short distances make multipath propagation the dominant effect in almost all the frequency range. Since PLC transmissions can be considered unfeasible when attenuation values are larger than 95 dB [53], it can be observed that the maximum length of actual links would be around 250 m.

[3]See corresponding maps at https://cutt.ly/AgEZbni and https://cutt.ly/bgECGCl, respectively

TABLE 4. Number of Channels (of each type) Considered in Each Topology.

Topology	Number of channels
Linear 1	126
Linear 2	84
Manhattan-like	55
Random 1	64
Random 2	116
Random 3	124
Random 4	84
Random 5	115
Random 6	186
Aurora avenue	215
SOHO	190
Total	1359

Fig. 5 also shows interesting differences between topologies. Surprisingly, the linear and Manhattan-like channels have similar characteristics for a given link length. The reason is that distances between derivations to street lights in the Manhattan-like topology (60 m) are so large that the multipath effect is masked by the conductor and dielectric losses. Hence, the SOHO topology actually reveals itself as the worst-case because of its highly branched structure with most street lights spaced around 12 m. For short link lengths ($\ell = 36$), the number of derivations from the main path from the transmitter to the receiver in the SOHO topology is still small and has little effect, as shown in Fig. 5. However, as the link length increases, so does the number of derivations and their effect in the channel response, particularly in the band below 20 MHz.

Given the low-pass behavior of OPLN channels, their amplitude response can be roughly modeled by means of a linear function whose slope and constant terms depend on the link length, ℓ,

$$|H(f)|\ (\text{dB}) \approx \Delta(\ell) f + \Omega(\ell), \tag{1}$$

with f in MHz, ℓ in meters and where $\Delta(\ell) = \alpha \cdot \ell + \beta$ and $\Omega(\ell) = a \cdot \ell + b$. The corresponding values of these parameters for each scenario can be obtained by firstly accomplishing a robust regression of each response vs frequency and then a robust regression of the parameters of the former vs the link length. Obtained results are shown in Table 5. As seen, α is very similar in all topologies, but significant differences occur

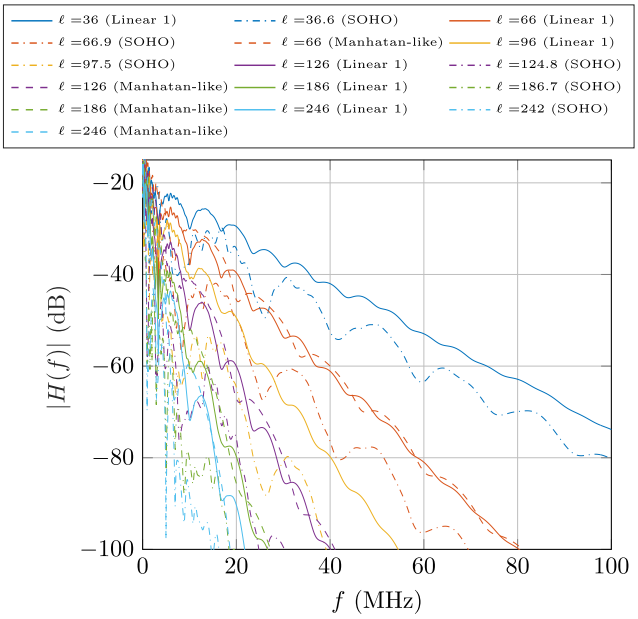

FIGURE 5. Amplitude of some representative SISO channels from the Linear 1, SOHO and Manhattan-like topologies with different link lengths.

TABLE 5. Parameters of the Robust Fit of the Amplitude of the Channels in the Considered Topologies.

Topology	$\alpha \cdot 10^3$	$\beta \cdot 10^3$	$a \cdot 10^3$	b
Linear 1	−14.9243	−3.1962	−56.9780	−17.6510
Linear 2	−14.3455	−39.9347	−101.8312	−16.6387
Manhattan-like	−15.1883	−5.1271	−35.3028	−16.9878
Random 1	−14.9374	−2.4616	−72.5238	−17.0738
Random 2	−14.7895	−14.8982	−76.9101	−18.2600
Random 3	−14.9274	−4.7343	−64.0914	−17.5107
Random 4	−14.9509	0.1036	−70.9507	−16.2184
Random 5	−14.9843	−0.327	−58.7607	−17.4866
Random 6	−14.8537	−8.7024	−72.2241	−17.4384
Aurora avenue	−14.5833	−29.0970	−123.6925	−16.8762
SOHO	−14.2763	−36.7121	−158.2547	−18.6179

in the a term (also in β, but its influence is much smaller), being the SOHO topology the worst-case.

A statistical analysis of the delay spread and the average attenuation of the SISO channels indicated in Table 4 has been obtained. Fig. 6 depicts a scatter plot of the average attenuation vs the link length in different frequency bands. The corresponding regression lines, given by Attenuation (dB) $= \delta \cdot \ell + \lambda$ with ℓ in meters, are also shown. The values of δ and λ for the different frequency bands are given in Table 6.

Fig. 6 can be helpful to determine the actual frequency band that could be used in a given link. Hence, it shows that is very unlikely that the frequency band above 40 MHz can be used in links larger than 150 m. It is also interesting to note that the dispersion of attenuation values decreases as the frequency increases (dots are more concentrated around the regression line). This is due to the larger influence of the conductor and dielectric losses in the attenuation as frequency increases.

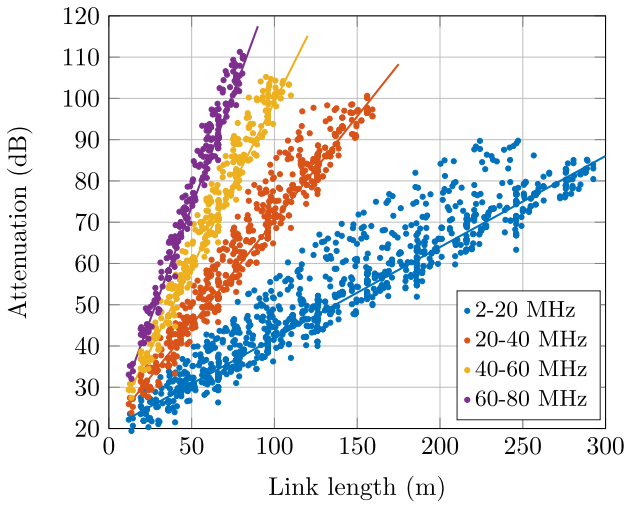

FIGURE 6. Scatter plot of the average attenuation of the SISO channels in different frequency bands vs the link length.

TABLE 6. Parameters of the Robust Fit of the Average Attenuation of the Channels in Different Frequency Bands.

Frequency band	δ	λ
2–20	0.2208	19.8053
20–40	0.5057	19.7905
40–60	0.8010	19.0161
60–80	1.0938	19.0428

Fig. 7 shows a scatter plot of the delay spread of the SISO channels vs the link length. Two frequency bands are considered, the one used by ITU-T G.hn and HomePlug AV2 devices (2–80 MHz) and by IEEE P1901 ones (2–50 MHz). Dispersion increases with the link length because the number of derivations from the main path from the transmitter to the receiver may take much different values in longer links than in shorter ones. Hence, in the latter case, differences among channels responses (of the same length) are smaller than in the former, as shown in Fig. 5. Delay spread values increase with the link length because the low-pass behavior of the channel response intensifies as the link length augments, which progressively concentrates the effective channel response to the low frequency region, as observed in Fig. 5. Since attenuation values in the band above 50 MHz are generally very large, the energy of the channel impulse response is essentially concentrated in the low frequency region, which makes delay spread values in the 2–80 MHz band to be almost equal to the ones in the 2–50 MHz. Finally, it is interesting to highlight that values shown in Fig. 7 are similar to the ones found in indoor PLC channels [62], [63]. This ensures than the cyclic prefix lengths of the state-of-the-art OFDM-based PLC systems shown in Table 3 are appropriate for this scenario.

Once the main features of the SISO channels have been presented, Fig. 8(a) depicts the responses of three representative 3 × 3 MIMO channels and Fig. 8(b) their corresponding

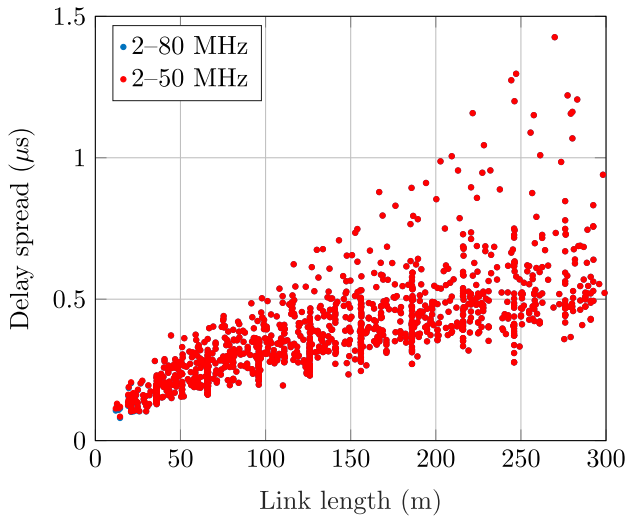

FIGURE 7. Scatter plot of the delay spread of the SISO channels vs the link length.

condition number, defined as [35, pp. 141]

$$\kappa(f) = 20\log_{10}\left(\frac{\max\{\sigma_i(f)\}}{\min\{\sigma_i(f)\}}\right), \tag{2}$$

where $\sigma_i(f)$ denotes the i-th singular value of the 3×3 MIMO channel matrix

$$\mathbf{H}(f) = \begin{bmatrix} H_{11}(f) & H_{12}(f) & H_{13}(f) \\ H_{21}(f) & H_{22}(f) & H_{23}(f) \\ H_{31}(f) & H_{32}(f) & H_{33}(f) \end{bmatrix}, \tag{3}$$

with $H_{ij}(f)$ being the channel frequency response between the i-th transmitting port and the j-th receiving port. As defined in (2), small values of κ denote low spatial correlation and, consequently, higher potential bit-rate gains compared to the SISO system.

It must be highlighted that, while the location of the transmitter and the receiver are the same as in the SISO case, the SISO response does not match either $H_{11}(f)$, $H_{22}(f)$ nor $H_{33}(f)$ because the conditions at the transmitter and receiver ports are different. In general, the less branched the path from the transmitter to the receiver is, the more similar the frequency responses of the MIMO channel are. This can be observed by noticing that the responses of MIMO channel in the linear topology are more alike than in the more branched SOHO scenario. As link length increases, so does the number of derivations, causing more notches in the low frequency band. This enlarges the condition number and the number of effective MIMO streams reduces. This is the case of the SOHO $\ell = 186.7$ curve shown in Fig. 8(b).

In order to assess the spatial correlation of the MIMO channels, Fig. 9 depicts the cumulative distribution function (CDF) of the gain of the three MIMO streams (i.e., the singular values of the MIMO matrices) computed over the whole set of channels and frequencies. The CDF of the amplitude response of the corresponding SISO channel is depicted as a reference. As seen, the gain of the first MIMO stream is generally about 10 dB larger than the one of the second stream

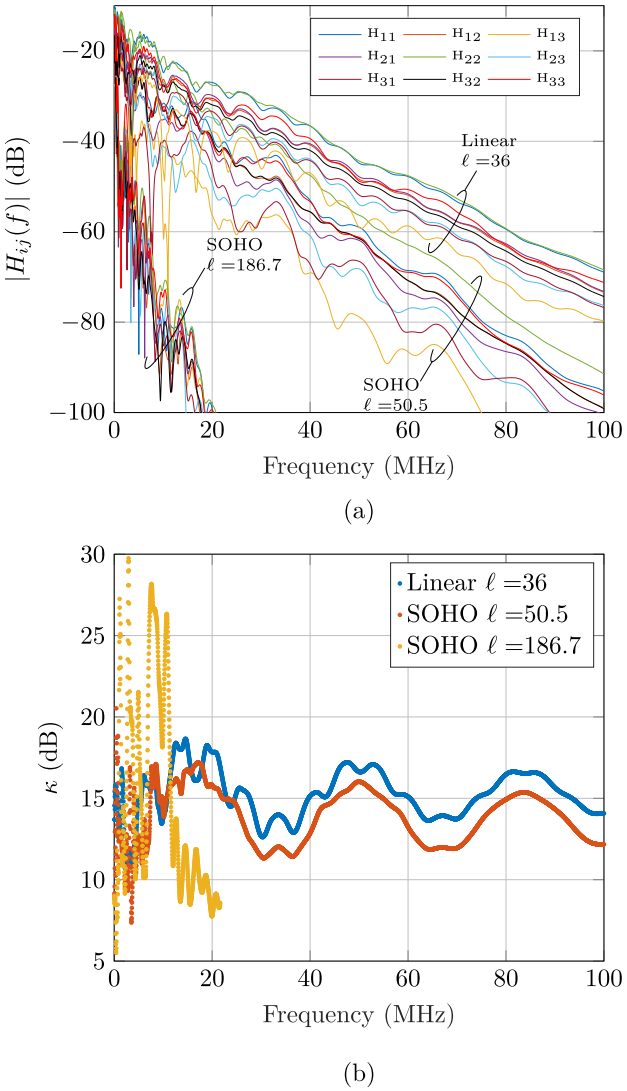

FIGURE 8. Amplitude response and condition number of some representative 3 × 3 MIMO channels from the Linear 1 and SOHO topologies with different link lengths.

and about 15 dB larger than the one of the third stream. As a reference, values up to 10 dB are generally considered very good (in terms of performance improvement with respect to the SISO system) while values larger than 20 dB are almost useless [64]. This allows foreseeing that MIMO techniques may report considerably bit-rate gains.

It must be noted that the cable model considered in this work assumes constant distance between conductors, as in the 4-pole cables conventionally used in OPLN in many countries. Interestingly, this results in lower spatial correlation than when the distance between conductors varies, like in monopolar cables, as shown in [65].

In contrast to the significant frequency selective behavior of the amplitude response, the gains of the resulting MIMO streams are quite frequency-independent, with slightly larger condition numbers in the frequency band below 20 MHz. However, a detailed analysis is omitted for the sake of conciseness.

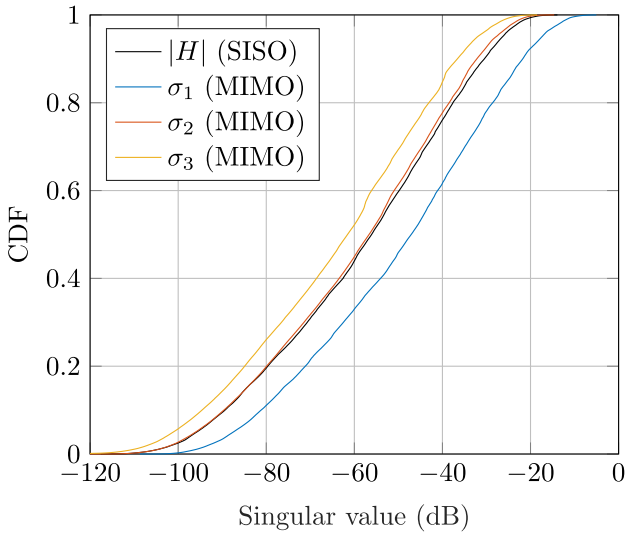

FIGURE 9. CDF of the singular values of the MIMO matrix and of the response of the SISO channel.

B. NOISE MEASUREMENTS

Results presented in this work have been extracted from measurements in OPLN of the city of Málaga (Spain) using the set-up described in [23]. Two networks with notably different characteristics have been selected to this end. One has a linear topology with 12 m lamp-post height, spaced between 45 m and 65 m, and lamps of 400 W. It is located in a residential district by the seafront, where noise is expected to be low. The measured circuit has 7 lamps. The other network has a quite branched topology and is located in the SOHO district, with a high density of office and residential buildings, which would presumably yield higher noise levels.[4] Distance between lamps-post ranges between 10 and 30 meters with 4 m and 8 m lamp-posts height. Shorter ones are equipped with 150 W lamps, while taller ones contain either a single 250 W lamp or two lamps, one with 250 W (at 8 m) and 150 W (at 4 m).

Fig. 10 depicts the noise PSD measured in four locations of the SOHO district when the three phases are active. Noticeably, noise at the control panel is much higher than at the base of any lamp-post. This is another reason (in addition to the low impedance of the FRS) to avoid using the control panel as a communication end point. Measurement (2) corresponds to a lamp-post with two lamps located at different heights (250 W and 150 W), while (3) and (4) correspond to lamp-post with a single 150 W lamp. It is observed that noise is lower in the latter. As in the indoor PLC scenario, noise is higher in the band below 30 MHz, except for the disturbance caused by the commercial FM radio broadcasting in the frequency band above 87 MHz. Similarly, there are many narrowband interference terms with considerably high level over the noise floor.

[4]See corresponding maps at https://goo.gl/8XzmZN -Carretera Nacional 340- and https://goo.gl/DeRqNA -Cordoba and Trinidad Grund streets-, respectively.

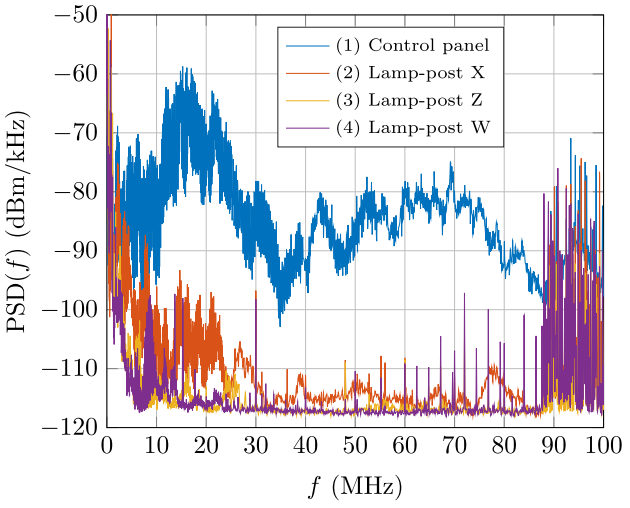

FIGURE 10. Noise PSD estimated from measurements at four locations of the SOHO. All phases active.

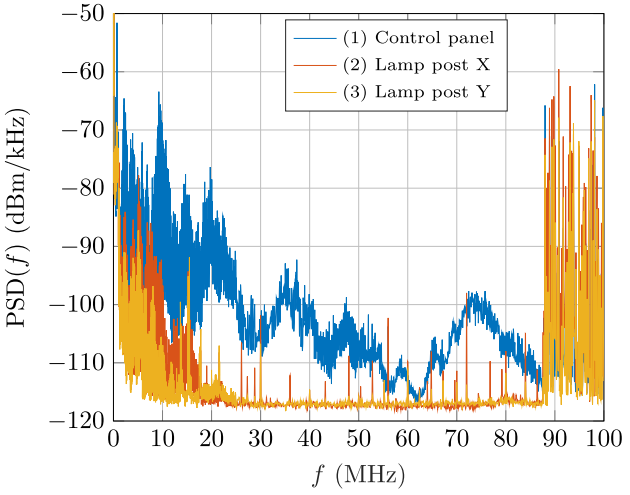

FIGURE 11. Noise PSD estimated from measurements at the seafront. Only one active phase.

Representative noise PSD measured at the seafront network with only one active phase are given in Fig. 11. It exhibits the same characteristics observed in the SOHO measurements. As expected, noise level are lower than in the latter. Differences are particularly observable in the control panel location.

To assess the influence of the number of active phases (among the three existing ones), Fig. 12 shows the noise PSD measured at some locations of the seafront network when all phases are active and when only one is active. Surprisingly, the noise level does not augments with the number of active phases, neither at the control panel nor at the base lamp. In fact, noise level is higher when only one phase is active.

It is interesting to note that the PSDs shown in Fig. 10 to Fig. 12 exhibit quite a strongly ripple in the low frequency region (in the control panel, this extends to almost the whole band). This is due to the periodic behavior of some noise

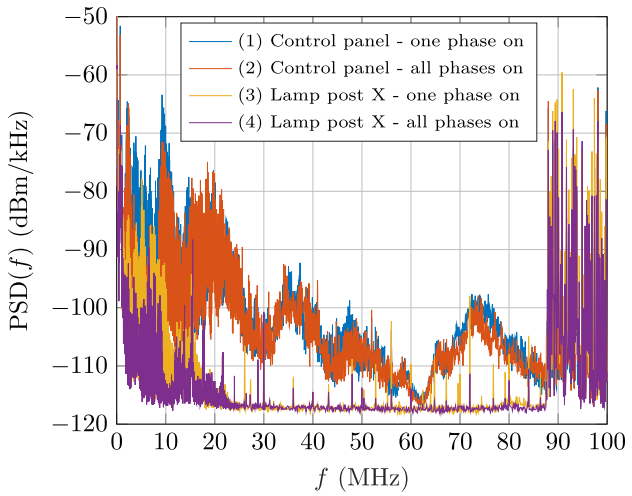

FIGURE 12. Noise PSD estimated from measurements at three locations of the seafront with different number of active phases.

terms, which is clearly illustrated in Fig. 13. The latter depicts the time-domain waveforms of some noise registers measured in the considered OPLN. As seen, they resemble the ones registered in indoor PLC scenarios [66]. The periodic envelope of these noise waveforms is mainly due to the cyclostationary behavior of many of the narrowband interference terms and to the impulsive periodic asynchronous with the mains components [66]. The latter, which can be clearly observed in Fig. 13(d), manifest in the PSD as very narrow peaks with frequency spacing equal to its repetition rate and are the responsible for the referred ripples in the PSD in the band below 30 MHz [66].

VI. PERFORMANCE ANALYSIS

This section firstly gives estimated throughput values obtained from simulations over the set of channels described in Section V. The study assumes a SISO and a 2 × 2 MIMO system with the parameters of the ITU-T G.hn given in Table 3. A 3 × 3 MIMO system with the same parameters of the ITU-T G.hn, except for the additional transmitter and receiver ports, is also considered. In MIMO cases, the transmitter power is optimally distributed among the streams [67, Sec. 10.3] and the noise is assumed to be uncorrelated between ports with the PSDs described in section V-B. This is actually a worst-case assumption, since measurements indicate that noise is considerably correlated in the band below 20 MHz and this can be exploited to improve the bit-rate by means of a whitening transformation [19].

Afterward, measured throughput, delay and jitter values obtained with ITU-T G.hn devices in three actual OPLN are given. Finally, potential performance enhancements given by techniques that are currently being investigated are summarized.

A. ESTIMATED PERFORMANCE

A statistical analysis of the throughput achieved over the set of modeled channel responses and measured noise PSD

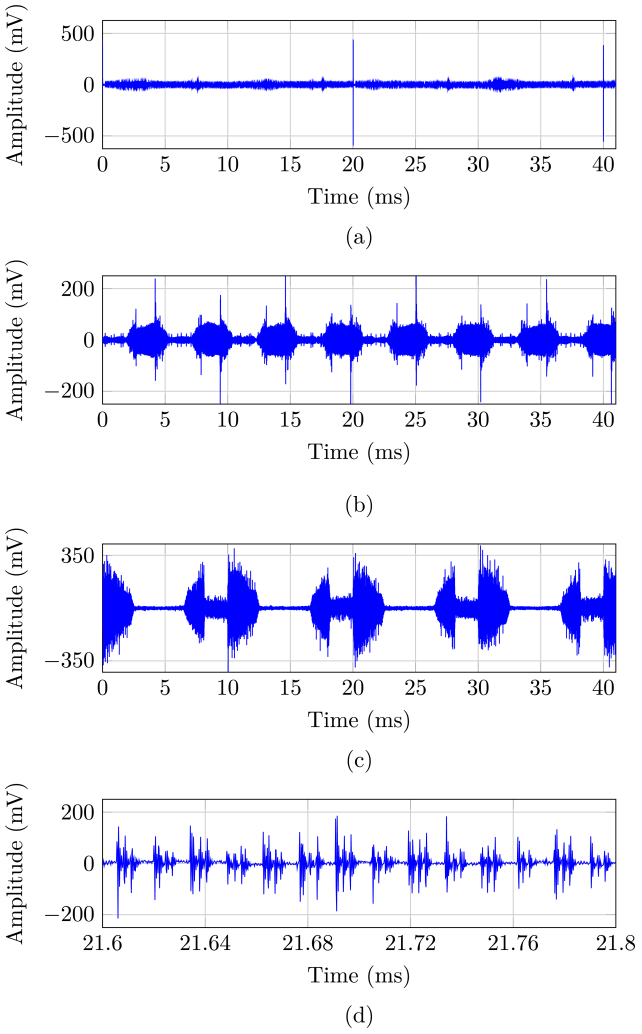

FIGURE 13. Noise waveforms exhibiting a cyclostationary behavior (a) in a lamp-post at the seafront; (b) in a lamp-post at the SOHO; (c) in the control panel at the seafront; (d) zoom of the waveform in (c).

has been obtained. The PSD mask of the transmitted signal is fixed according to the ITU-T Rec. G.9964, including all permanent frequency notches. The latter reduce the number of useful carriers to 3317 and yield a maximum PHY SISO bit-rate of 740.4 Mbit/s. This value assumes continuous OFDM symbol transmission and takes into account neither interframe gaps imposed by the MAC nor the overhead of this layer and the upper ones. In order to assess the feasibility of PLC as a backhaul technology, throughput values at UDP level have to be obtained, as it is the transport protocol used in the connection to the S-GW [28]. While the relation of the latter to the PHY bit-rate depends on many factors, assuming that only two devices are present and that the transmission is unidirectional, the UDP throughput can be assumed to be 62.2% of the PHY bit-rate [53].

Fig. 13 depicts a scatter plot of the estimated SISO UDP throughput vs the link length in two noise conditions. The bounding curves (dashed lines) are given by UDP throughput (Mbit/s) $= ae^{-b\ell}$, with ℓ being the link length in meters and with a and b as given in Table 7. The

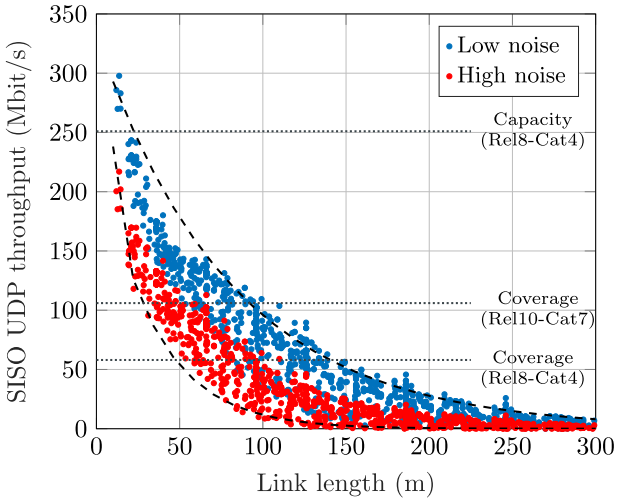

FIGURE 14. Scatter plot of the estimated SISO UDP throughput vs the link length for two noise levels.

TABLE 7. Parameters of the Bounding Curves of the SISO UDP Throughput Region.

Curve	a	b
Upper bound	329.4	0.01185
Lower bound	287.7	0.03466

throughput required by the backhaul cases given in Table 2 are also shown, except for the capacity (Rel.10-Cat.7) one, which is much higher than the achieved values. As seen, the dispersion of values increases as the throughput decreases. Hence, while high throughput values are only attained in short links, the range of link lengths with low throughput values is much larger. It can also be observed that the backhaul required by the capacity (Rel.8-Cat.4)-driven small cell deployments can be provisioned only in very short links with low noise conditions.

Since attenuation of OPLN PLC channels is very high in the band above 40 MHz, as shown in Fig. 6, and the PSD mask above 30 MHz is 30 dB lower than in the low frequency band, it is interesting to assess the actual throughput improvement provided by the frequency band above 50 MHz, which is the upper frequency used by IEEE P1901. To this end, Fig. 15 depicts the ratio of the throughput of a SISO system in the frequency band up to 86 MHz, denoted as SISO-100 MHz in the G.hn terminology, compared to a SISO system using the frequency band up to 50 MHz. As seen, only very short links benefit from the use of the upper frequency band. Hence, from this perspective, the ITU-T G.hn and the IEEE P1901-OFDM will perform similarly. However, the latter does not include MIMO techniques which, as will be shown below, may give considerably performance improvements.

To estimate the probability of attaining a certain throughput for a given link length, Fig. 16 shows the complementary cumulative distribution function (CCDF) of the SISO UDP throughput for various link length ranges under two noise conditions. The throughput required for the reference use

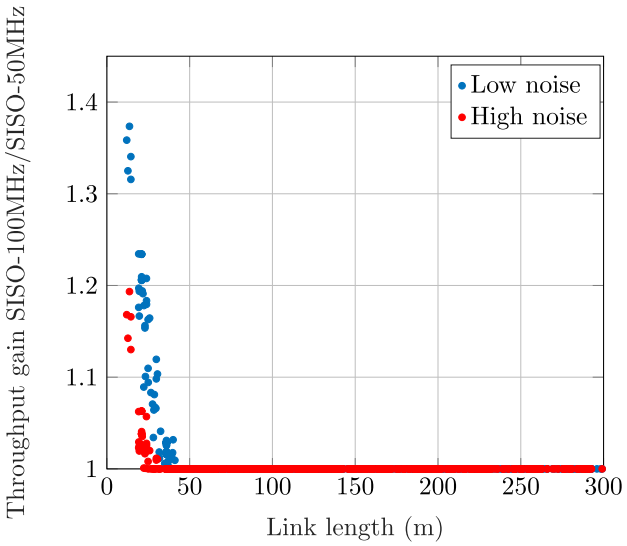

FIGURE 15. Scatter plot of the throughput gain of the SISO-100MHz system with respect to the SISO-50MHz one vs link length.

cases are also depicted, except for the capacity (Rel.10-Cat.7) one. As observed, the throughput value required by the coverage (Rel.8-Cat.4) use case can be provisioned in almost all links in the range 50–100 m when the noise level is low and in approximately 60% of the links when the noise level is high. For links with length 100–150 m, the required throughput can be provided to 50% of the links when noise level is low. The coverage (Rel.10-Cat.7) use case can be served in all links shorter than 50 m and in about 60% of the links with length 50–100 m in low noise conditions. On the other hand, the percentage of capacity (Rel.8-Cat.4) scenarios that can be served is almost negligible. When the noise level is high, the considered system is unable to provide the throughput required by the coverage (Rel.10-Cat.7) use case to links longer than 50 m and the one of the coverage (Rel.8-Cat.4) case to links longer than 100 m.

Now the performance improvement given by MIMO techniques is assessed. Fig. 17(a) shows the CCDF of the throughput gain (defined as the ratio of the considered values) of the 3×3 MIMO system with respect to the SISO system and to the 2×2 MIMO conventionally used in the ITU-T G.hn. The gain of the latter with respect to the SISO is also shown. As seen, the improvements with respect to the SISO system are notable: median gain is around 2.6 for the 3×3 MIMO (about 2 for the 2×2 MIMO) and 90% of the links experience gains larger than 2.3 (1.8 for the 2×2 MIMO). Gains of the 3×3 MIMO with respect to the 2×2 MIMO of current ITU-T G.hn devices are more modest, but still notable, as the median gain is around 1.25 and 10% of the links experience throughput ratios larger than 1.4. The improvement is generally larger in the low noise scenario, except for very attenuated channels. In the latter, the throughput of the baseline systems is very low (or almost zero) and, despite throughput values achieved by the 3×3 MIMO are also small, the relative gain is very high. This effect is magnified by the quantization of the number of

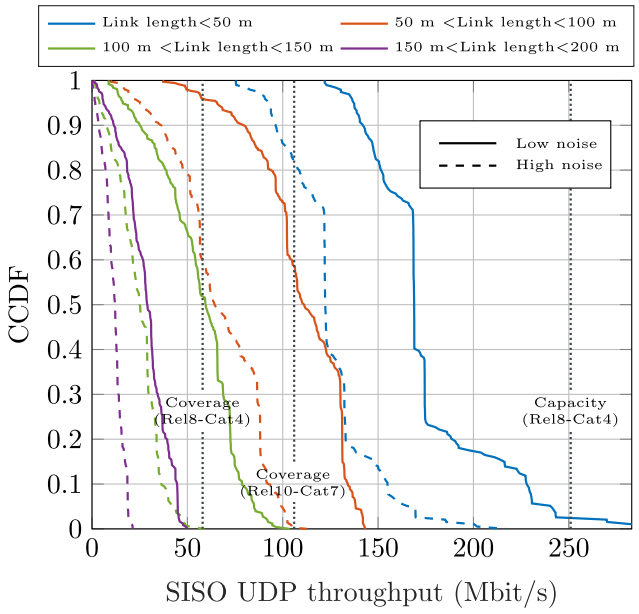

FIGURE 16. CCDF of the estimated SISO UDP throughput for different link lengths.

TABLE 8. Parameters of the Bounding Curves of the UDP Throughput Region of the 3 × 3 MIMO System.

Curve	a	b
Upper bound	878.4	0.0126
Lower bound	708.7	0.03127

bits per symbol due to the constellations defined in the ITU-T Rec. G.hn.

To assess the distribution of the throughput gain with respect to the link length, Fig. 17(b) depicts a scatter plot of the throughput gain of the 3 × 3 MIMO with respect to the 2 × 2 MIMO system vs the link length. As seen, increasing the link length reduces the gains and increases the dispersion. The throughput gains lower than 1 observed in long links, which are due to the quantization of the number of bits per symbol, occur because the same MIMO order has been employed in all carriers. This is a worst-case assumption, as the optimum transmission strategy (3 × 3 MIMO, 2 × 2 MIMO or single-input multiple-output) could be selected on a per-carrier basis.

Fig. 18(a) depicts a scatter plot of the estimated UDP throughput of the 3 × 3 MIMO system vs the link length in two noise conditions. The throughput required for the reference use cases are also depicted. The bounding curves (dashed lines) are given by UDP throughput (Mbit/s) $= ae^{-b\ell}$, with ℓ being the link length in meters and the values of a and b as given in Table 8. The throughput required by the backhaul cases given in Table 2 are also shown. Fig. 18(b) shows the CCDF of the corresponding throughput values for various links length ranges. As seen, while the throughput considerably improves with respect to the SISO case depicted in Fig. 14 (×2.3 in 90% of the links), it is still

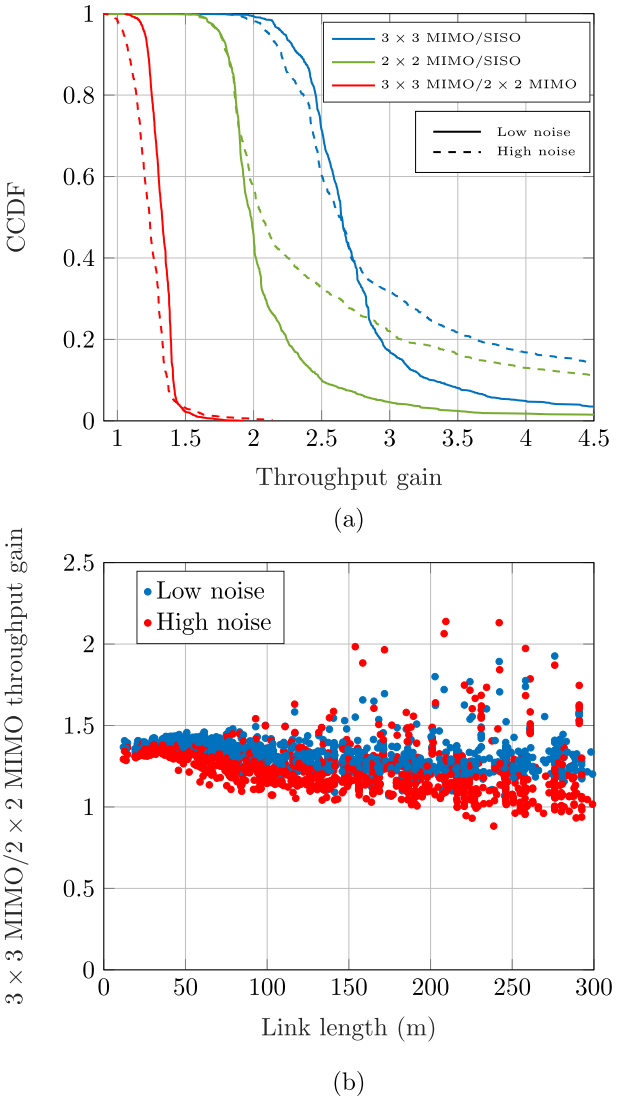

FIGURE 17. (a) CCDF of the throughput gain of the MIMO 3 × 3 with respect to the 2 × 2 MIMO and the SISO systems and of the 2 × 2 MIMO with respect to the SISO; (b) Scatter plot of the throughput gain of the 3 × 3 MIMO with respect to the 2 × 2 MIMO vs the link length.

very unlikely that the throughput required by the capacity (Rel.10-Cat.7) use case can be provided, even in short links. However, the capacity (Rel.8-Cat.4) use case can be served in 90% of the links of up to 50 m, even with high noise level. The coverage (Rel.10-Cat.7) use case can be served in more than 80% of the links in the range 50–100 m when noise level is high and about 80% of the links with length in the range 100–150 m when noise level is low. Finally, the least demanding case, the coverage (Rel.8-Cat.4), can be served in about 95% of the links with length 100–150 m and in 70% of the links with length 150–200 m when the noise level is low. It must be emphasized that the referred throughput values are irrespective of the type of backhaul link, LOS or NLOS, which is irrelevant in PLC. The latter is particularly common in small cell deployments in the center of European cities.

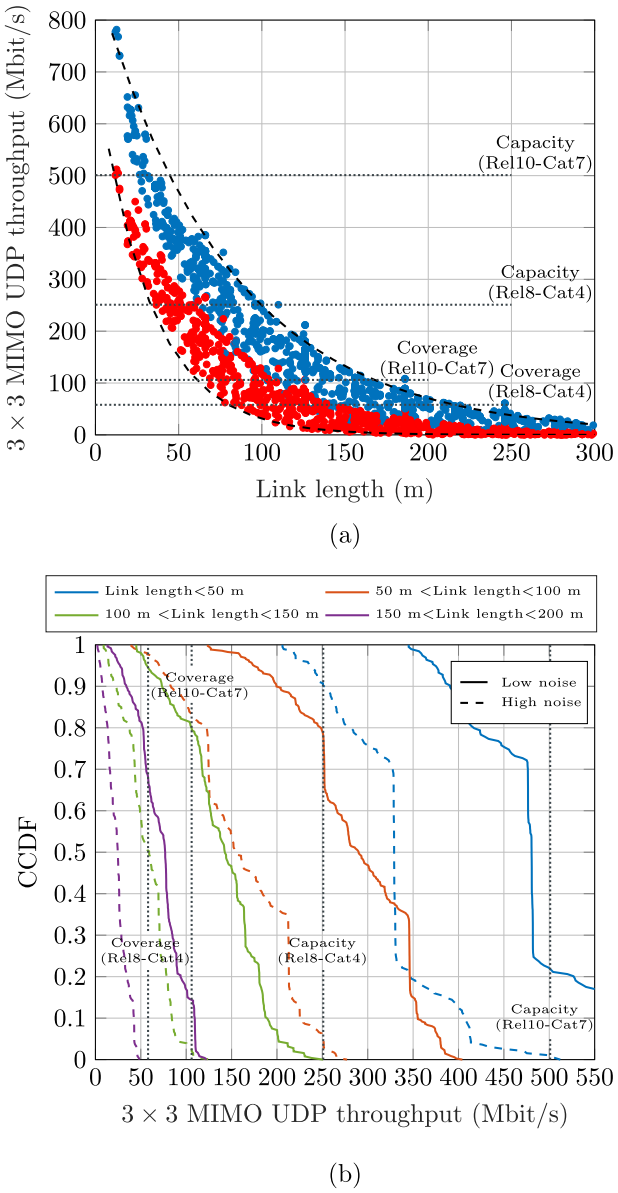

FIGURE 18. (a) Scatter plot of the estimated UDP throughput of the 3 × 3 MIMO system vs link length; (b) CCDF of the estimated 3 × 3 MIMO UDP throughput for different link lengths.

Comparing the obtained values with the ones provided by alternative backhaul technologies described in [11], it is noticeable that they are similar to the ones given by some Sub-6 GHz wireless solutions in NLOS conditions and by wired ones like G.fast (note that the values in [11, Table 2] are theoretical ones). Compared to the latter, the PLC backhaul will have a much lower operative cost.

B. MEASURED PERFORMANCE

Performance in live OPLN has been assessed by trials using ITU-T G.hn devices featuring the Marvell 88LX3142 (digital baseband processor) and 88LX2718 (analog front end) chipsets. These have three working modes: 50 MHz SISO, 100 MHz SISO and 50 MHz MIMO, attaining a maximum PHY bit-rate of 800 Mbit/s. Employed devices are designed for indoor PLC scenarios, where the root mean square voltage between the phase and neutral is 240 V, while maximum voltage between any two phases of the OPLN is about 400 V. Hence, the conductor connected to the protective earth port has been left open circuit at the control panel (no mains signal), to prevent damaging the devices, and only the 100 MHz SISO mode has been used.

Three tests have been performed: the throughput and round trip delay ones defined in the RFC 2544 [68], the jitter test specified in the RFC 3393 [69] and a bidirectional transport control protocol (TCP) throughput test. The latter is accomplished using the PassMark Performance Test v8.0 software tool [70], while the JDSU Smart Class Ethernet Tester is used for the former [71]. The RFC 2544 throughput test begins by sending frames at the maximum theoretical rate of the port. The frame rate is adjusted until no frame loss occurs. It can be performed for different MAC frame sizes ranging from 64 to 1518 bytes. However, since the duration of a test in actual conditions is about 2 hours for a given frame size, only the one corresponding to 64 bytes has been carried out. This provides a lower bound of the performance, as it is the most stressing test for the device, which has to transmit a larger number of frames to convey the same data volume. Additionally, the PHY bit-rates registered by a proprietary software tool from the chipset manufacturer are given to allow the comparison with the estimated results given in the previous subsection.

Table 9 summarizes the results obtained in the two scenarios described in Section V-B. The RFC 2544 and RFC 3393 tests correspond to a single direction, which can be referred to as DL. However, the TCP and PHY rates are also given for the UL. Since the 64-byte length is actually a worst case, an estimation of the layer 1 (L1) values, according to the RFC 2544 denomination, that would be obtained using 1518-byte frames are also given in brackets. The extrapolation has been computed taking the laboratory test given in [53] as a reference.

As expected, the highest throughput values are attained in the seafront scenario, which has a linear topology. In the two links of this scenario, the L1 throughput for 1518-byte frames is larger than the minimum one required for a coverage-driven (Rel.8-Cat.4) small cell deployment. Even for 64-byte frames, the attained throughput in the longest link is about the needed one and larger enough in the 51 m one. In the SOHO networks, the L1 throughput for 64-byte frames is almost the one required by the coverage (Rel.10-Cat.7) use case in link 6 and larger than the one of the coverage (Rel.8-Cat.4) in link 7. For the 1518-byte frames, the demanded throughput can be loosely provided in both links. The comparison of the throughput attained in links 6, 7 and 8 illustrates the dispersion of performance values for a given link length that has already been observed in Fig. 14 and Fig. 16.

Overall, the ITU-T G.hn devices are able to provide the required throughput for the coverage-driven (Rel.8-Cat.4)

TABLE 9. Measured Performance Values Using ITU-T G.hn Devices in 100 MHz SISO Mode.

Link #	Scenario	Link length (m)	PHY bit-rate (Mbit/s) [UL|DL]	TCP throughput (Mbit/s) [UL|DL]	RFC 2544 L1 throughput[a] (Mbit/s)	RFC 2544 Round trip delay (ms)	RFC 3393 Jitter (μs) [mean|max]
1	Seafront	102	112|123	45.01|51.83	52.48 (71.90)	18.820	0|1016
2	Seafront	51	219|104	58.12|49.89	66.84 (91.57)	16.747	0|1147
3	SOHO[b]	140	19|23	7.72|8.69	1.22 (1.67)	61.539	721|12780
4	SOHO	96	47|56	4.94|13.39	14.34 (19.65)	41.296	33|9535
5	SOHO[b]	80	40|35	17.88|13.87	12.90 (17.67)	23.487	66|10781
6	SOHO[b]	30	265|229	55.20|93.72	105.57 (144.63)	9.830	0|10027
7	SOHO[b]	30	184|152	54.17|72.65	62.96 (86.25)	6.352	0|9667
8	SOHO	28	106|88	38.82|43.50	26.57 (36.40)	7.268	0|9470

[a] Measured values for 64-byte frames (in brackets, extrapolated ones for 1518-byte frames).

[b] Streetlights with light emitting diode (LED) technology lamps.

small cell scenario in links of up to 100 m. In a highly branched topology, provisioning is only feasible in much shorter links. Provisioning for the coverage (Rel.10-Cat.7) use case is possible only in some very short links. However, it must be emphasized that these values have been measured using the 100 MHz SISO mode; better performance is expected using the 2×2 MIMO mode with appropriate protection at the coupling circuit (simulated median gain shown in Fig. 17 is 2) and even larger by employing a 3×3 MIMO scheme. Moreover, additional gains can be envisaged by including some of the potential improvements discussed later in Section VI-C.

Measured delay values fulfill the requirements of the most restrictive service shown in Table 2 (gaming) in all cases except link 3, where it is slightly exceeded. Average jitter values are negligible and maximum ones are about 10 ms, which is lower than the 30 ms limit recommended for voice over internet protocol (VoIP) services [72, Ch.2].

Table 9 reveals that DL TCP throughput values are generally similar or even larger than the L1 ones for 64-byte frames, despite TCP is located three layers above the PHY and is a connection-oriented protocol. The reason is that the L1 throughput is determined for 0% frame loss and the 64-byte length is actually a worst case. Hence, the L1 throughput can be taken as a conservative estimate of the UDP throughput in an actual scenario (the performance loss due to the MAC, internet protocol (IP) and UDP headers are negligible for the 1518-byte frames). To compare these measured values with the ones estimated by means of simulations in Section VI-A, Fig. 19 depicts the L1 throughput measured with the 100 MHz SISO using the 64-byte frames and the estimated values for the 1518-byte frames. The UDP throughput region obtained from simulations is depicted as a reference. As seen, except for the values corresponding to link 8, measured and simulated results fit quite well.

To further assess the validity of the estimations obtained by means of simulation in Section VI-A, the UL and DL PHY bit-rate values reported by the chipset manufacturer (which are computed assuming similar simplifications) in the

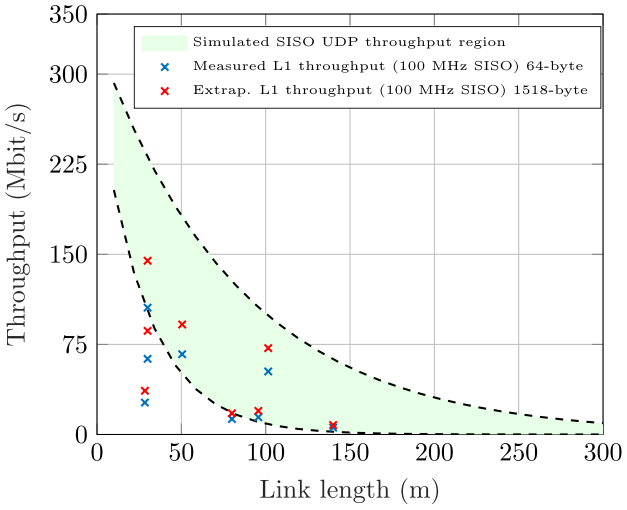

FIGURE 19. Measured L1 throughput for 64-byte frames and estimated for 1518-byte frames in the 100 MHz SISO mode and simulated UDP throughput region vs distance.

100 MHz SISO mode are presented in Fig. 20. The region corresponding to the simulated values is shaded in green. As seen, most of the reported values fall within the region predicted by simulation. This endorses the need for using a statistical approach to estimate the performance of PLC systems even when the bottom-up modeling is employed. Traditionally, the ability to estimate the response of a particular channel in a deterministic way has been argued as one of the positive features of this channel modeling strategy. However, this requires precise knowledge of the underlying topology and cable characteristics. While the former could be obtained from the network schemes of the municipalities, the experience gained during this work shows that these schemes may contain errors, e.g., some derivations or lamps are not reflected, or maybe outdated because of constructions that forced to make temporary changes that finally became permanent. Most important, schemes do not usually show the phase to which lamps are connected, which is of great importance for estimating the channel response.

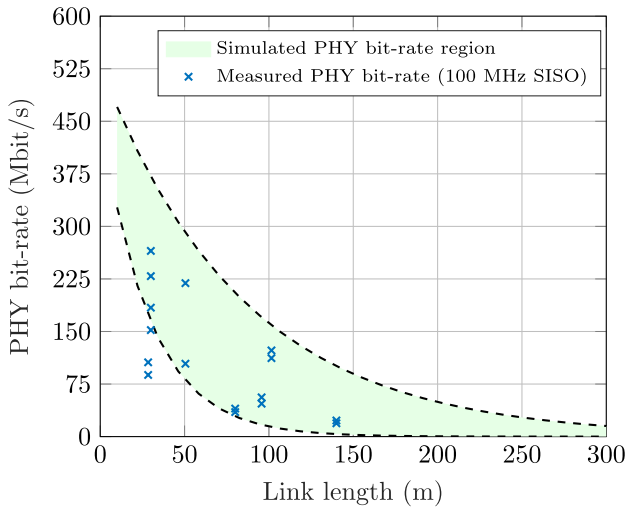

FIGURE 20. Measured (UL and DL) and simulated PHY bit-rate vs distance.

C. POTENTIAL PERFORMANCE IMPROVEMENTS

This subsection briefly describes some promising techniques that are currently being investigated and the expected performance enhancement they can provide. It must be mentioned that reported values corresponding to MIMO systems have been obtained for the conventional 2×2 system currently used in indoor scenarios. Additionally, other enhancements not discussed here, such as flexible spectrum management, multilevel coding and variable interframe gap, are considered in the ITU-T G.hn2 standard that is currently being developed and that is aimed at enhancing the maximum PHY bit-rate of the ITU-T G.hn by approximately 2.7 times (from 1.5 Gbit/s to 4 Gbit/s) [21].

1) IN-BAND FULL DUPLEX (IBFD)

IBFD can potentially double the PHY bit-rate by allowing simultaneous transmission and reception in the same frequency band and conductors [20]. IBFD does not only improves the PHY bit-rate, but also the throughput at the logical link control (LLC) sublayer. Accordingly, IBFD has been proposed as a study-item for the upcoming ITU-T G.hn2 [73], [74].

The PHY bit-rate gain given by IBFD depends on the relative power of the uncancelled interference from the transmitter with respect to the signal of interest and the noise levels. Mercifully, IBFD provide larger gains in channels with large attenuation and high noise level than in channels lowly attenuated and with low noise level. Published results indicate that IBFD improves the PHY bit-rate by at least 1.6 times in SISO receivers. In MIMO receivers the bit-rate is doubled in 70% of the channels in high noise conditions and median gains are larger than 1.8 when noise level is low [75]. These figures correspond to in-home PLC channels but similar gains can also be expected in outdoor channels, since they are usually more attenuated and with similar or even higher noise levels than indoor ones [23].

2) RELAYING CAPABILITIES

Multi-hop communications have been longly proposed as a means to improve the performance of PLC in highly attenuated in-home and outdoor channels [76]–[78]. These proposals have explored the performance gains obtained with decode-and-forward (DF) and amplify-and-forward (AF) schemes in systems using time division duplexing (TDD), where the bit-rate is halved in each hop.

The use of IBFD may considerably increase the relaying capacity of PLC systems, since relays can receive and transmit simultaneously [20]. Interestingly, to achieve this end, relays are the only network elements that must have the IBFD functionality [79]. This feature is particularly interesting for the application considered in this work, since it can enhance the relaying capacity of PLC systems, extending the maximum length of the backhaul link.

Accordingly, the use of an AF relay with IBFD capability has been recently proposed [80]. Obtained results indicate that the proposed relay can double the bit-rate of the direct communication when the SNR $= 10$ dB, and up to ten times when SNR $= -10$ dB. To this end, frequency selective amplification and impedance adaptation at the hybrid are required. When simpler schemes are used, the maximum gains are more modest, but improvements of about 2 times larger than the direct link can be attained in long links [81].

The use of IBFD, both at the communications end and at the relying devices, may considerably improve the performance of PLC systems given in Fig. 18. Hence, an enhancement of $\times 2$ would allow providing the capacity required in the capacity (Rel.10-Cat.7) use case in almost all links shorter than 50 m, even with a high noise level; it would also allow provisioning for the capacity (Rel.8-Cat.4) use case in links of up to 100 m and the coverage (Rel.8-Cat.4) in almost all links shorter than 200 m with low noise conditions.

3) NOISE REDUCTION/EXPLOITATION TECHNIQUES

Noise is likely the most serious impairment in PLC. It has been mainly combated by incorporating stronger coding schemes that do not exploit its particularities, namely, its cyclostationary non-Gaussian nature and the correlation between ports in MIMO systems. Noise cancellation strategies that leverage gains from the sparse nature of major noise components, e.g., of the impulsive terms in the time and of the narrowband interference in the frequency domain could report notable gains [82]. Similarly, the work in [18], which provides upper and lower bounds for the capacity of SISO and MIMO PLC channels for different noise models, has shown that the Gaussian assumption classically made in PLC is generally very pessimistic, specially at medium to high SNR.

VII. CONCLUSION

This article has assessed the feasibility of using PLC over OPLN as a backhaul technology for outdoor small cell deployments. To this end, PLC channels established over OPLN have been first characterized by combining noise measurements in actual networks and channel responses

obtained using an MTL model. Results show that the delay spread of the channels is much lower than the cyclic prefix of state-of-the-art OFDM-based PLC systems, which makes them suitable for this scenario, and that the frequency response in the band above 50 MHz is dominated by the attenuation due to the skin effect in links larger than 50 m.

The performance of PLC systems is assessed by means of simulations and complemented with measurements in actual networks. The latter show that PLC can fulfill the delay requirements, while simulated results show that a 3×3 MIMO system can provide the throughput required by coverage-driven small deployments with backhaul length of up to 100–150 m, depending on the considered LTE release. Compared to existing backhaul solutions, achieved performance is similar to some existing Sub-6 GHz wireless solutions in NLOS conditions and to wired ones like G.fast.

Moreover, the future ITU-T G.hn2 standard, currently under development, is expected to further improve the performance of current systems. Additional enhancements can be obtained by including noise reduction/exploitation techniques and IBFD functionality, both at the communications ends and at intermediate relying devices.

These facts suggest that PLC might be a feasible solution for backhauling certain outdoor small cells scenarios. Following steps to validate this end should evaluate the availability of PLC connections by exhaustively assessing the stability of throughput, delay and jitter values. Noise level variation is expected to be the main source of performance instability. It must be emphasized that other backhaul technologies are also affected by specific sources of instability, e.g., microwave wireless systems are prone to link outage caused by blockages and atmospheric absorption due to heavy rain. Similarly, the most appropriate method to have the small cell BS synchronized in frequency with the mobile network is yet to be investigated.

ACKNOWLEDGMENT

The authors thank Vodafone Group Services Limited, Manuel Salazar (Head of the Servicios Operativos of the City Council of Málaga), Monelec S.L. and Marvell Hispania (now MaxLinear Hispania) for the support provided to this work.

REFERENCES

[1] Ericsson. (Jun. 2020). *Ericsson Mobility Report*. [Online]. Available: https://www.ericsson.com/en/mobility-report/reports/june-2020

[2] Cisco. (Mar. 2020). *Cisco Annual Internet Report (2018-2023)*. [Online]. Available: https://bit.ly/2K6pixj

[3] J. Lee, Y. Kim, Y. Kwak, J. Zhang, A. Papasakellariou, T. Novlan, C. Sun, and Y. Li, "LTE-advanced in 3GPP REL-13/14: An evolution toward 5G," *IEEE Commun. Mag.*, vol. 54, no. 3, pp. 36–42, Mar. 2016.

[4] B. Bojović, L. Giupponi, Z. Ali, and M. Miozzo, "Evaluating unlicensed LTE technologies: LAA vs LTE-U," *IEEE Access*, vol. 7, pp. 89714–89751, 2019.

[5] N. Bhushan, J. Li, D. Malladi, R. Gilmore, D. Brenner, A. Damnjanovic, R. T. Sukhavasi, C. Patel, and S. Geirhofer, "Network densification: The dominant theme for wireless evolution into 5G," *IEEE Commun. Mag.*, vol. 52, no. 2, pp. 82–89, Feb. 2014.

[6] Document 049.07.02, Small Cell Forum. (Feb. 2013). *Backhaul Technologies for Small Cells: Use Cases, Requirements and Solutions*. [Online]. Available: https://bit.ly/2ItNrNI

[7] M. Kamel, W. Hamouda, and A. Youssef, "Ultra-dense networks: A survey," *IEEE Commun. Surveys Tuts.*, vol. 18, no. 4, pp. 2522–2545, 4th Quart., 2016.

[8] M. Ding, D. López-Pérez, H. Claussen, and M. A. Kaafar, "On the fundamental characteristics of ultra-dense small cell networks," *IEEE Netw.*, vol. 32, no. 3, pp. 92–100, May 2018.

[9] M. Paolini, L. Hiley, and F. Rayal. (2013). *Small-Cell Backhaul: Industry Trends and Market Overview*. [Online]. Available: https://bit.ly/3mZUeO1

[10] (Aug. 2018). *Small Cell Siting Challenges and Recommendations*. [Online]. Available: https://bit.ly/3oFH1dX

[11] M. Jaber, M. A. Imran, R. Tafazolli, and A. Tukmanov, "5G backhaul challenges and emerging research directions: A survey," *IEEE Access*, vol. 4, pp. 1743–1766, 2016.

[12] A. H. Jafari, D. López-Pérez, H. Song, H. Claussen, L. Ho, and J. Zhang, "Small cell backhaul: Challenges and prospective solutions," *EURASIP J. Wireless Commun. Netw.*, vol. 2015, no. 1, pp. 1–18, Dec. 2015.

[13] M. Mahloo, P. Monti, J. Chen, and L. Wosinska, "Cost modeling of backhaul for mobile networks," in *Proc. IEEE Int. Conf. Commun. Workshops (ICC)*, Jun. 2014, pp. 397–402.

[14] M. Martínez, "G.hn technology for industrial and smart grid applications. ITU-T roadmap and HomeGrid Forum certification update," in *Proc. IEEE Int. Symp. Power Line Commun. Appl. (ISPLC)*, May 2020, pp. 1–27. [Online]. Available: https://bit.ly/3n1CO3A

[15] C. Cano, A. Pittolo, D. Malone, L. Lampe, A. M. Tonello, and A. G. Dabak, "State of the art in power line communications: From the applications to the medium," *IEEE J. Sel. Areas Commun.*, vol. 34, no. 7, pp. 1935–1952, Jul. 2016.

[16] *IEEE Standard for Medium Frequency (less than 12 MHz) Power Line Communications for Smart Grid Applications* Standard 1901.1, May 2018.

[17] MaxLinear Document. (Oct. 2020). *2Gbps G.hn MAC/PHY Transceiver Solutions for Networking over Powerlines, Phone Lines and Coaxial Cable*. [Online]. Available: https://cutt.ly/AgTYYqW

[18] N. Shlezinger, R. Shaked, and R. Dabora, "On the capacity of MIMO broadband power line communications channels," *IEEE Trans. Commun.*, vol. 66, no. 10, pp. 4795–4810, Oct. 2018.

[19] J. A. Cortés, J. A. Corchado, F. J. Cañete, and L. Díez, "Analysis and exploitation of the noise correlation in MIMO power line communications in the FM band," *IEEE Commun. Lett.*, vol. 22, no. 3, pp. 566–659, Dec. 2018.

[20] G. Prasad, L. Lampe, and S. Shekhar, "In-band full duplex broadband power line communications," *IEEE Trans. Commun.*, vol. 64, no. 9, pp. 3915–3931, Sep. 2016.

[21] M. Martínez and S. Iranzo. (Apr. 2019). *G.hn Standardization: Present and Future*. [Online]. Available: https://bit.ly/2ndqLXx

[22] F. Marcuzzi and A. M. Tonello, "Stochastic geometry for the analysis of small radio cells and PLC back-hauling," in *Proc. Int. ITG Conf. Syst., Commun. Coding*, 2017, pp. 1–6.

[23] J. A. Cortés, F. J. Cañete, M. Toril, L. Díez, and A. García-Mozos, "Analysis of power line communications for last-hop backhaul in small cells deployment," in *Proc. IEEE Int. Symp. Power Line Commun. Appl. (ISPLC)*, Apr. 2019, pp. 1–6.

[24] A. Maeder, M. Lalam, A. De Domenico, E. Pateromichelakis, D. Wübben, J. Bartelt, R. Fritzsche, and P. Rost, "Towards a flexible functional split for cloud-RAN networks," in *Proc. Eur. Conf. Netw. Commun. (EuCNC)*, Jun. 2014, pp. 1–5.

[25] J. Bartelt, P. Rost, D. Wübben, J. Lessmann, B. Melis, and G. Fettweis, "Fronthaul and backhaul requirements of flexibly centralized radio access networks," *IEEE Wireless Commun.*, vol. 22, no. 5, pp. 105–111, Oct. 2015.

[26] *LTE; Evolved Universal Terrestrial Radio Access (E-UTRA) and Evolved Universal Terrestrial Radio Access Network (E-UTRAN); Overall description; Stage 2*, document ETSI TS 136 300 V9.4.0 (2010-07), European Telecommunications Standards Institute (ETSI), Jul. 2010.

[27] NGMN white paper. NGMN Alliance. (Jun. 2012). *Small Cell Backhaul Requirements*. [Online]. Available: https://bit.ly/39ShauX

[28] *3GPP Evolved Packet System (EPS); Evolved General Packet Radio Service (GPRS) Tunnelling Protocol for Control plane (GTPv2-C); Stage 3*, document TS 29.274 version 15.4.0 Release 15, 3GPP, Jul. 2018.

[29] J. Wannstrom. (Jun. 2013). *LTE-Advanced*. [Online]. Available: https://bit.ly/2VURiqb

[30] *Policy and Charging Control Architecture (Release 16)*, document TS 23.203 V16.2.0, 3GPP, Dec. 2019. [Online]. Available: https://bit.ly/33YsXnI

[31] *LTE; Scenarios and Requirements for Small Cell Enhancements for E-UTRA and E-UTRAN*, document TR 36.932 version 16.0.0 Release 16) ETSI TR 136 932 V16.0.0, European Telecommunications Standards Institute (ETSI), 3GPP, Jul. 2020.

[32] Real Wireless Ltd. (Feb. 2014). *The Business Case for Urban Small Cells*, Small Cell Forum, Rep. [Online]. Available: https://bit.ly/2K05mfn
[33] *Backhaul for Urban Small Cells: A Topic Brief*, document 095.07.03, Small Cell Forum, Jun. 2015. [Online]. Available: https://bit.ly/36YKvCn
[34] L. Yonge, J. Abad, K. Afkhamie, L. Guerrieri, S. Katar, H. Lioe, P. Pagani, R. Riva, D. M. Schneider, and A. Schwager, "An overview of the HomePlug AV2 technology," *J. Electr. Comput. Eng.*, vol. 2013, pp. 1–20, Dec. 2013.
[35] L. T. Berger, A. Schwager, P. Pagani, and D. M. Scheneider, Eds., *MIMO Power line Communications: Narrow and Broadband Standards, EMC and Avanced Processing*, 1st ed. Boca Raton, FL, USA: CRC Press, 2014.
[36] L. Lampe, A. M. Tonello, and T. G. Swart, Eds., *Power Line Communications: Principles, Standards and Applications from Multimedia to Smart Grid*, 2nd ed. Hoboken, NJ, USA: Wiley, Jun. 2016.
[37] K. H. Afkhamie, S. Katar, L. Yonge, and R. Newman, "An overview of the upcoming HomePlug AV standard," in *Proc. Int. Symp. Power Line Commun. Appl.*, 2005, pp. 400–404.
[38] HomePlug Alliance. (Feb. 2014). *HomePlug AV Specification Version 2.1*. [Online]. Available: https://bit.ly/39YvjXB
[39] *Standard for Broadband Over Power Line Networks: Medium Access Control and Physical Layer Specifications* Standard P1901, Jun. 2010.
[40] *Unified High-Speed Wireline-Based Home Networking Transceivers—System Architecture and Physical Layer Specification*. document G.9960, ITU-T Recommendation, Jul. 2015.
[41] *Data Link Layer (DLL) for Unified High-Speed Wire-Line Based Home Networking Transceivers*, document G.9961, Telecommunications Union, Jun. 2010.
[42] *Unified High-Speed Wireline-Based Home Networking Transceivers—Multiple Input/Multiple Output Specification*, document ITU-T Recommendation G.9963, International Telecommunications Union, Dec. 2011.
[43] *Unified High-Speed Wireline-Based Home Networking Transceivers—Power Spectral Density Specification*, document ITU-T Recommendation G.9964, International Telecommunications Union, Dec. 2011.
[44] *Coexistence Mechanism for Wireline Home Networking Transceivers*, document ITU-T Rec. G.9972, International Telecommunications Union, Jun. 2010.
[45] M. Rindchen, "An overview on global power line standards and European EMC certification," in *Proc. 9th Workshop Power Line Commun.*, Sep. 2015, pp. 1–15.
[46] *The Impact of Power Line High Data Rate Telecommunication Systems on Radiocommunication Systems Below 470 MHz*, document ITU-R Recommendation SM.1879-2, International Telecommunications Union, Aug. 2013.
[47] M. Navarro. (Dec. 2017). *Status of EMC (Electromagnetic Compatibility) Regulation (FCC/EU) for G.hn Powerline, Coax and Phoneline Devices*. [Online]. Available: https://bit.ly/2VVTRIM
[48] L. T. Berger, A. Schwager, P. Pagani, and D. M. Schneider, "MIMO power line communications," *IEEE Commun. Surveys Tuts.*, vol. 17, no. 1, pp. 106–124, 1st Quart., 2015.
[49] *Power Line Communication Apparatus Used in Low-Voltage Installations—Radio Disturbance Characteristics—Limits and Methods of Measurement—Part 1: Apparatus for in-Home Use*, document EN 50561-1, Comité Européen de Normalisation Electrotechnique (CENELEC), Oct. 2013.
[50] *Power Line Communication Apparatus Used in Low-Voltage Installations—Radio Disturbance Characteristics—Limits and Methods of Measurement—Part 3: Apparatus Operating Above 30 MHz*, document EN 50561-3:2016, Comité Européen de Normalisation Electrotechnique (CENELEC), 2016.
[51] (Feb. 2014). *Directive 2014/30/EU of the European Parliament and of the Council of 26 February 2014, On the Harmonisation of the Laws of the Member States Relating to Electromagnetic Compatibility*. [Online]. Available: https://bit.ly/36V9Lcy
[52] M. Koch. (Mar. 2016). *EU Regulation of High-Speed Powerline Communication in the Spectrum 150-500 kHz*. [Online]. Available: https://bit.ly/37NXPs9
[53] (Oct. 2018). *Wave-2 Powerline Networking Evaluation Public User Guide*. [Online]. Available: https://bit.ly/3qHncEU
[54] *PowerLine Telecommunications (PLT); Basic Data Relating to LVDN Measurements in the 3 MHz to 100 MHz Frequency Range* , document ETSI TR 102 370 V1.1.1, ETSI, Nov. 2004.
[55] *Guía Técnica de Aplicación de la ITC-BT-09: Instalaciones de Alumbrado Exterior*, Ministerio de Industría Comercioy Turismo, Madrid, Spain, 2004.
[56] *Anexo 2 de la Guía Técnica de Aplicación de la ITC-BT-09: Instalaciones de Alumbrado Exterior*, Ministerio de Industría Comercioy Turismo, Madrid, Spain, 2004.
[57] J. I. Urraca and I. Urraca, *Instalaciones de Alumbrado Exterior. Guía Técnica de Aplicación Ampliaday Comentada*. Madrid, Spain: Asociación Española de Normalización y Certificación, 2005.
[58] D. G. Kendall, "Branching processes since 1873," *J. London Math. Soc.*, vols. s1–41, no. 1, pp. 385–406, 1966.
[59] C. R. Paul, *Analysis of Multiconductor Transmission Lines*. Hoboken, NJ, USA: Wiley, 1994.
[60] F. Versolatto and A. M. Tonello, "An MTL theory approach for the simulation of MIMO power-line communication channels," *IEEE Trans. Power Del.*, vol. 26, no. 3, pp. 1710–1717, Jul. 2011.
[61] J. A. Corchado, J. A. Cortés, F. J. Cañete, and L. Díez, "An MTL-based channel model for indoor broadband MIMO power line communications," *IEEE J. Sel. Areas Commun.*, vol. 34, no. 7, pp. 2045–2055, Jul. 2016.
[62] M. Tlich, A. Zeddam, F. Moulin, and F. Gauthier, "Indoor power-line communications channel characterization up to 100 MHz—Part II: Time-frequency analysis," *IEEE Trans. Power Del.*, vol. 23, no. 3, pp. 1402–1409, Jul. 2008.
[63] A. M. Tonello, F. Versolatto, and A. Pittolo, "In-home power line communication channel: Statistical characterization," *IEEE Trans. Commun.*, vol. 62, no. 6, pp. 2096–2106, Jun. 2014.
[64] H. Mellein and M. Mielkech. (Aug. 2017). *Assessing a MIMO Channel*. [Online]. Available: https://bit.ly/3mqpbdW
[65] J. A. Corchado, J. A. Cortés, F. J. Cañete, A. Arregui, and L. Díez, "Analysis of the spatial correlation of indoor MIMO PLC channels," *IEEE Commun. Lett.*, vol. 21, no. 1, pp. 40–43, Jan. 2017.
[66] J. A. Cortés, L. Díez, F. J. Cañete, and J. J. Sánchez-Martínez, "Analysis of the indoor broadband power-line noise scenario," *IEEE Trans. Electromagn. Compat.*, vol. 52, no. 4, pp. 849–858, Nov. 2010.
[67] A. Goldsmith, *Wireless Communication*. New York, NY, USA: Cambridge Univ. Press, 2005.
[68] S. Bradner and J. McQuaid, *Benchmarking Methodology for Network Interconnect Devices*, document RFC 2544, Internet Request for Comments, Mar. 1999.
[69] C. Demichelis, *IP Packet Delay Variation Metric for IP Performance Metrics (IPPM)*, document RFC 3393, Internet Request for Comments, Nov. 2002.
[70] PassMark Software. *Passmark Performance Test v8.0*. Accessed: Aug. 2020. [Online]. Available: https://cutt.ly/rgTOcdy
[71] Product Description. *JDSU Smart Class Ethernet Tester*. Accessed: Aug. 2020. [Online]. Available: https://cutt.ly/GgTOHCB
[72] T. Szigeti and C. Hattingh, *End-to-End QoS Network Design: Quality of Service in LANs, WANs, and VPNs*. San Jose, CA, USA: Cisco, 2004.
[73] D. Kim, H. Lee, and D. Hong, "A survey of in-band full-duplex transmission: From the perspective of PHY and MAC layers," *IEEE Commun. Surveys Tuts.*, vol. 17, no. 4, pp. 2017–2046, 4th Quart., 2015.
[74] G. Prasad and L. Lampe, "Full-duplex power line communications: Design and applications from multimedia to smart grid," *IEEE Commun. Mag.*, vol. 58, no. 2, pp. 2–8, Jan. 2019.
[75] G. Prasad, L. Lampe, and S. Shekhar, "Digitally controlled analog cancellation for full duplex broadband power line communications," *IEEE Trans. Commun.*, vol. 65, no. 10, pp. 4419–4432, Oct. 2017.
[76] S. D'Alessandro and A. M. Tonello, "On rate improvements and power saving with opportunistic relaying in home power line networks," *EURASIP J. Adv. Signal Process.*, vol. 2012, no. 1, pp. 1–17, Dec. 2012.
[77] X. Cheng, R. Cao, and L. Yang, "Relay-aided amplify-and-forward power-line communications," *IEEE Trans. Smart Grid*, vol. 4, no. 1, pp. 265–272, Mar. 2013.
[78] K. M. Rabie and B. Adebisi, "Enhanced amplify-and-forward relaying in non-Gaussian PLC networks," *IEEE Access*, vol. 5, pp. 4087–4094, 2017.
[79] E. Antonio-Rodríguez, S. Werner, R. López-Valcarce, T. Riihonen, and R. Wichman, "Wideband full-duplex MIMO relays with blind adaptive self-interference cancellation," *Signal Process.*, vol. 130, pp. 74–85, Jan. 2017.
[80] F. Passerini and A. M. Tonello, "Analog full-duplex amplify-and-forward relay for power line communication networks," *IEEE Commun. Lett.*, vol. 23, no. 4, pp. 676–679, Apr. 2019.
[81] F. J. Cañete, G. Prasad, and L. Lampe, "PLC networks with in-band full-duplex relays," in *Proc. IEEE Int. Symp. Power Line Commun. Appl. (ISPLC)*, May 2020, pp. 1–6.
[82] D. Shrestha, A. M. Tonello, X. Mestre, and M. Payaró, "Simultaneous cancellation of narrow band interference and impulsive noise in PLC systems," in *Proc. IEEE Int. Conf. Smart Grid Commun. (SmartGridComm)*, Nov. 2016, pp. 326–331.

JOSÉ ANTONIO CORTÉS (Member, IEEE) received the M.S. and Ph.D. degrees in telecommunication engineering from the Universidad de Málaga, Spain, in 1998 and 2007, respectively. In 1999, he was with Alcatel España Research and Development. In 1999, he joined the Communication Engineering Department, Universidad de Málaga, where he became an Associate Professor in 2010. From 2000 to 2002, he collaborated with the Nokia System Competence Team, Málaga. From 2014 to 2016, he was on a leave of absence working as a Consultant on the development of Atmel's power line communications (PLC) solutions. His research interests include digital signal processing for communications, mainly focused on channel characterization and transmission techniques for PLC. He was the General Co-Chair of the IEEE ISPLC 2020. He is an Associate Editor of the IEEE Open Journal of the Communications Society and the IEEE Communications Letters, where he has been recognized as an Exemplary Editor in 2019 and 2020. He has been serving as a Secretary for the IEEE Communications Society Technical Committee on Power Line Communications, since 2018.

FRANCISCO JAVIER CAÑETE (Senior Member, IEEE) received the M.S. and Ph.D. degrees in telecommunication engineering from the Universidad de Málaga (UMA), Spain, in 1996 and 2004, respectively. In 1996, he was with the Instrumentation and Control Department, INITEC, in the design of power plants. In 1997, he worked for the Research and Development Department, Alcatel, Spain, in the design of wireless local loop systems. Since 1998, he has been with the Communication Engineering Department, UMA, where he is currently an Associate Professor. In 2000 and 2001, he also collaborated with the Nokia System Competence Team, Málaga, in 3G radio resource management. He served as the Head for the Communication Engineering Department and also the Deputy Vice-Chancellor for Academical Organization, both at UMA, and also a Secretary for the IEEE Communications Society Power Line Communications Technical Committee. His current research interests include signal processing for digital communications with special interest in channel modeling and transmission techniques for wireless systems, underwater acoustic communications, and power line communications.

MATÍAS TORIL received the M.S. and Ph.D. degrees in telecommunication engineering from the Universidad de Málaga, Spain, in 1995 and 2007, respectively. Since 1997, he has been a Lecturer with the Communications Engineering Department, Universidad de Málaga, where he is currently a Full Professor. He has coauthored more than 150 publications in leading conferences and journals and 8 patents owned by Nokia Corporation and Ericsson. His current research interests include self-organizing mobile networks, radio resource management, and data analytics.

EDUARDO MARTOS-NAYA received the M.Sc. and Ph.D. degrees in telecommunication engineering from the Universidad de Málaga, Málaga, Spain, in 1996 and 2005, respectively. In 1997, he joined the Department of Communication Engineering, Universidad de Málaga, where he is currently an Associate Professor. His research interests include digital signal processing for communications, channel estimation, synchronization and performance analysis, and the channel modeling of wireless systems.

JAVIER PONCELA received the M.Sc. degree in telecommunications engineering from the Polytechnic University of Madrid, Madrid, Spain, in 1994, the Ph.D. degree in telecommunications engineering from the University of Málaga, Spain, in 2009, and the M.B.A. degree from the University of Málaga, in 2011. He did his Ph.D. research on methodologies for efficient development of complex communications systems. He has actively collaborated with multinational companies (Nokia, Cetecom GmbH, AT4wireless, and Ingenia) on formal modeling and system testing in Bluetooth, 3G, and satellite systems. Since 2012, he has been serving as the Deputy Dean for International Relations in ETSIT. He also coordinates international Mobility Programs Erasmus+ KA107 between University of Málaga and Universities in Pakistan and France. He has been a Coordinator of the Master on Telematics and Communication Networks for 6 years. He was with Alcatel Spacio before joining the Universidad de Málaga, in 1997, where he is currently an Associate Professor. He is also a Co-Founder of the Applied Communications Engineering for Underwater Research and Development Group. He has participated in more than ten research projects, coauthoring more than 50 publications, 23 of them in JCR journals. His research interests include underwater communication networks, analysis of end-to-end performance, and models for the evaluation of QoE. He has been a Co-Editor of special issues in Wireless Personal Communications.

LUIS DÍEZ received the M.S. and Ph.D. degrees in telecommunications engineering from the Polytechnic University of Madrid, Spain, in 1989 and 1995, respectively. From 1987 to 1997, he was an Assistant Professor with the Department of Signals, Systems and Radiocommunication, Polytechnic University of Madrid. Since 1997, he has been with the Department of Communications Engineering, Universidad de Málaga, where he is currently an Associate Professor. His research interests include digital communication, a field in which he has worked for many years. His experience includes most of its applications, such as voiceband, DSL, and cable modems; satellite, mobile, and power line communications; and technical aspects, such as synchronization, adaptive signal processing, modulation, coding, and multiple access.

ALICIA GARCÍA received the M.S. degree in telecommunications engineering from the University of Malaga, Spain, in 2007. She spent the early years of her career in AT4 Wireless (now Keysight) working in the requirements definition of radio certification systems for WiMax and LTE technologies. In 2009, she joined Vodafone Group Technology, Newbury, U.K., where she participated in the LTE trials to evaluate access performance and in 2011 lead the definition of a disruptive deployment strategy for Vodafone access networks using HetNet and innovative last-mile solutions in response of the mobile data explosion. In 2012, she moved to Vodafone Global Enterprise in the area of new product development where she managed the portfolio of in-building communication solutions (LAN/WLAN and 3G/4G Small Cells). She joined Fon, Madrid, in 2017, where she led the strategy of the new Enterprise portfolio of WiFi location-based services. Since February 2020, she has been a part of the Amazon Business Tech Team.